1   **Predicting Soil Salinity Using Machine Learning and Assessing Farmers' Adaptive Capacity: A**

2   **Study in the Red River Delta**

3   Huu Duy Nguyen[1], Dinh Kha Dang[2], Thi Anh Tam Lai[1], Duc Dung Tran[3], Himan Shahabi[4], Quang-

4   Thanh Bui[1]

5   [1] Faculty of Geography, VNU University of Science, Vietnam National University, Ha Noi, 334 Nguyen
6   Trai, Thanh Xuan district, Hanoi City, Vietnam; nguyenhuuduy@hus.edu.vn;
7   laithianhtam_t65@hus.edu.vn; thanhbq@vnu.edu.vn

8   [2] Faculty of Hydrology, Meteorology, and Oceanography, VNU University of Science, Vietnam National
9   University, Ha Noi, 334 Nguyen Trai, Thanh Xuan district, Hanoi, Vietnam; dangdinhkha@hus.edu.vn

10   [3] National Institute of Education, Nanyang Technological University, Singapore, Singapore; [4] Earth
11   Observatory of Singapore and Asian School of the Environment, Nanyang Technological University,
12   Singapore, Singapore; [5] Center of Water Management and Climate Change, Institute for Environment and
13   Resources, Vietnam National University, Ho Chi Minh City, Viet Nam; dungtranducvn@yahoo.com

14   [4] Departments of Geomorphology, Faculty of Natural Resources, University of Kurdistan,
15   Sanandaj City, Kurdistan Province, Iran; h.shahabi@uok.ac.ir

16   Corresponding: Huu Duy Nguyen (nguyenhuuduy@hus.edu.vn)

17   **Abstract**

18   Soil salinity is a grave environmental threat to agricultural development and food security in large parts of the world,

19   especially in the situation of global warming and sea level rise. Reliable information on the adaptive capacity of farms

20   plays a key role in reducing the socioeconomic effects of soil salinization and helps policymakers and farmers propose

21   more appropriate measures to combat the phenomenon. The research aims to design a theoretical framework to assess

22   soil salinity and farmers' adaptive capacity based on machine learning, optimization algorithms (namely, Xgboost

23   (XGB), XGB-Pelican Optimization Algorithm (POA), XGB-Siberian Tiger Optimization (STO), XGB-Serval

24   Optimization Algorithm (SOA), XGB-Particle Swarm Optimization (PSO), and XGB-Grasshopper Optimization

25   Algorithm (GOA)), remote sensing, and interviews with local people. We evaluated the geographical distribution of

26   soil salinity by applying machine learning to Sentinel 1 and 2A. The adaptive capacity of farmers was evaluated

27   through interviews with 87 households. The statistical indices, namely the mean absolute error (MAE), the root mean

28   square error (RMSE), and the correlation coefficient (R^2), were used to assess the machine learning models. The

29   outcome of this study demonstrated that all optimization algorithms were successful in improving the accuracy of the

30   XGB model. The XGB-POA had the most performance, with an R^2 value of 0.968, followed by XGB-STO (R^2=0.967),

31   XGB-SOA (R^2=0.966), XGB-PSO (R^2 = 0.964), and XGB-GOA (R^2=0.964), respectively. The soil salinity map

32   produced by the proposed models also indicated that the coastal and riverside regions were the most affected by soil

33   salinity. The results also showed human and financial resources to be the two most important factors influencing the

34   adaptive capacity of farmers. This study provides a key theoretical framework that enhances previous previous and

35   can assist policymarkers and farmers in managing land resource, such as accurately identifying areas affected by soil

36   salinity for agricultural development in the context of climate change. In addition, this research highlights the

37   importance of integrating machine learning, remote sensing, and socio-economic surveys in soil salinity management,

38   which can support farmers for sustainable agricultural development.

39   **Keywords:** Red river, soil salinity, machine learning, adaptive capacity

40   **1. Introduction**

41   Soil salinity is among the greatest threats to land management, posing significant problems to agricultural progress

42   and global food security (He et al., 2024; Jia et al., 2024; Xiao et al., 2024). According to FAO, soil salinity affects

43   about 424 million hectares of land surface (with a depth of 0-30 cm) and more than 833 million hectares of subsoil

44   (30-100 cm). This area is increasing by about 2 million hectares each year and influences more than 100 countries

45   worldwide, causing damage between 12 and 27.3 billion USD (Aksoy et al., 2024; Jia et al., 2024).

46   The soil salinity problem will occur at the local, regional, and global levels (Bandak et al., 2024; Liu et al., 2024). In

47   Vietnam, many littoral regions are affected by soil salinity problems. According to the 2021 Ministry of Agriculture

48   and Environmental Report on the Current Situation and Planning of Agricultural Development, in 2020, about 200,000

49   hectares of cropland in Vietnam were already affected by soil salinity. This problem is increasingly serious in Mekong

50   Delta and Red River Delta - home to over 40 million people and playing a key role in Vietnam's agricultural and

51   aquaculture sectors - where they account for 71% of paddy cultivation, 86% of aquatic farming, and 65% of fruit

52   production (General Statistics Office, 2024; Ministry of Aquaculture, Agriculture and Rural Development, 2013).

53   Because these low-lying coastal areas (Hung and Larson, 2014) are experiencing subsidence (Le Dang et al., 2014),

54   and declining river water levels,, they have become highly susceptible to the effects of climate variability and sea-

55   level rise (Dasgupta et al., 2009). Therefore, monitoring soil salinity is essential to inform agricultural management

56   strategies to ensure food security at local and regional levels.

57 In order to address the problem, it is important to have the most precise and current data on soil salinity. Traditionally,

58 direct field measurements of soil salinity yielded the most accurate data (Eldeiry et al., 2008; Rhoades and Ingvalson,

59 1971). This method collects point samples in the areas of interest one by one, which is time-consuming and requires

60 significant manual work. Although this method can accurately identify soil salinity, it requires many field missions to

61 collect the data over time, which can be time-consuming and resource-intensive. To reduce these limitations and obtain

62 continuous spatial data (such as raster data) suitable for GIS analysis and environmental monitoring, several studies

63 have used freely available remote sensing data, such as Landsat and Sentinel images. These data provide spatial (10m)

64 and temporal (3 to 5 days) resolution and capture multiple spectral bands (Asfaw et al., 2018; Cullu, 2003). Several

65 studies have demonstrated the effectiveness of remote sensing to monitor soil salinity accurately and rapidly. By

66 constructing correlations between remote sensing-derived indices and soil salinity points in the field, such as NDVI,

67 VSSI, and NDSI, we can achieve this. Although remote sensing can monitor soil salinity using different spectral

68 responses, slightly or moderately saline soils cannot be distinguished easily because soil minerals and their

69 components modify the spectral capacity of the soil surface.

70 Recently, with improvements in computing power, machine learning, and deep learning, there has beensubstantial

71 growth in techniques to construct soil salinity maps with higher accuracy. Algorithms such as random forest (Fathizad

72 et al., 2020), XGBoost (Jia et al., 2024), support vector machines (Jiang et al., 2019), CatBoost (Gong et al., 2023;

73 Wang et al., 2022), and AdaBoost (Wang et al., 2022) are the most popular algorithms to construct soil salinity maps

74 by integrating satellite images and in situ measurements. Some research has used deep learning models to construct

75 soil salinity maps, such as deep neural networks, recurrent neural networks, and Deep Boltzmann machines. Kaplan

76 et al. (2023) used four machine learning algorithms, namely M5P, RF, Linear, and IBK, integrated with Sentinel 2A

77 data and 393 soil samples collected in situ to construct a soil salinity map for the United Arab Emirates. The study's

78 results indicated that all models' performed well in assessing soil salinity, with the IBK model demonstrating the

79 highest effectiveness. Aksoy et al. (2024) used XGBoost and random forest with 26 environmental covariates from

80 Landsat 8 OLI to evaluate soil salinity in Iran's Lake Urmia. The study's outcome showed that machine learning

81 integrated with Landsat 8 OLI data successfully monitored soil salinity, with XGB yielding more accurate results than

82 random forest. Jia et al. (2024) applied nine models, namely PLSR, Lasso, CART, RF, ERT, GBDT, LightGBM,

83 XGBoost, and AdaBoost, integrated with Sentinel 2A imagery, to evaluate soil salinity in the Ningxia Yellow River

84 Diversion Irrigation Area. The results showed that the AdaBoost model performed better than the others.

85 Previous studies show that although machine learning methods have been utilized to assess soil salinity in many

86 regions of the world, their application for this purpose is still limited in the Mekong and Red River Deltas (Shi et al.,

87 2021; Vermeulen and Van Niekerk, 2017). Currently, there are only four studies that have assessed soil salinity in the

88 Mekong Delta (Hoa et al., 2019; Nguyen et al., 2023; Nguyen et al., 2018; Nguyen et al., 2021), and no work has been

89 done in this field for the Red River Delta. In addition, most previous studies have developed state-of-the-art methods,

90 such as integrating machine learning and remote sensing, to identify the geographical distribution of soil salinity in

91 different regions of the world (Hardie and Doyle, 2012; Su et al., 2020; Wang et al., 2007). While several studies have

92 highlighted the importance of assessing the adaptation capacity of the community to strengthen their resilience to soil

93 salinity and other types of natural hazards, however, very few studies integrate this aspect into the identification of

94 spatial soil salinity..Hoang et al. (2023) reported that assessing the ability of farms to adapt to soil salinization is the

95 key to reducing vulnerability and contributes significantly to the development of sustainable livelihoods.

96 The adaptive capacity is defined as the capability of the community to cope, adjust, and adapt to the impacts of growing

97 soil salinity. It measures the ability to predict, respond, and recover from the phenomenon. It is assessed on different

98 scales, using different approaches, according to the region in question (Mazumder and Kabir, 2022; Thiam et al.,

99 2024). Furthermore, understanding the adaptive capacity of communities plays an important role in reducing the

100 negative effects of salinity intrusion in coastal regions in general and the Red River Delta in particular. By assessing

101 adaptation at multiple scales with site-specific methods, researchers and local governments can identify interventions

102 (such as crop variety changes, crop calendars, irrigation systems) that are effective. The IPCC in 2014 indicated that

103 farm adaptive capacity depends on five main factors: natural capital, human capital, material resources, financial

104 resources, and social capital. Therefore, integrating the adaptive capacity of populations with the soil salinity map

105 improves the accuracy of predictions and proposes adaptation strategies that strengthen the overall resilience of

106 communities.

107 The research aims to improve a theoretical framework to assess soil salinity and farmers' adaptive capacity based on

108 machine learning, optimization algorithms (namely XGB, XGB- POA, XGB- STO, XGB- SOA, XGB- PSO, and

109 XGB- GOA), remote sensing, and interviews with local people. Several studies have examined farmer's adaptive

110 capacity to environmental stressors in different regions (Bhuyan et al., 2024; Thiam et al., 2024). However, no studies

111 comprehensively analyze farmers' adaptive ability to combat soil salinity in a given region based on machine learning,

remote sensing, and interviews with local people. In addition, several studies combine machine learning with Sentinel 1 or Sentinel 2 to assess soil salinity (Wang et al., 2021; Xiao et al., 2023); however, there are rarely studies that combine machine learning with Sentinel 1 and Sentinel 2 to monitor soil salinity in the Red River Delta. By the combination of Sentinel 1 and Sentinel 2, advanced machine learning, and the information from farmers themselves, this study filled a critical gap and provided a novel, comprehensive framework for monitoring and responding to soil salinity in the Red River Delta (Ma et al., 2021).

In general, salinity intrusion harms agricultural development and people's livelihoods. Therefore, it is necessary to develop a theoretical framework to address the soil salinity problem in terms of natural and social factors. However, previous studies have mainly assessed the spatial distribution of salinity or the community's adaptive capacity, and hardly any studies have assessed both the spatial distribution of salinity and the community's adaptive capacity. Thus, the global contribution of this study is to fill the knowledge gap about the spatial distribution of soil salinity and the adaptive capacity of communities in the Red River Delta in general and Thai Binh Province in particular by relying on modern methods to improve this important and understudied understanding. The results of this study can play an important role in mitigating the impact of salinity intrusion on agricultural development and can help policymakers and planners develop effective strategies to mitigate this impact, especially in the context of climate change.

2. Study Area

The Red River Basin covers a total area of 169,000 km² and spans China (48%), Laos (0.7%), and Vietnam (51.3%). The river system has a total length of 1,150 km, with around 500 km in the territory of Vietnam before discharging into the Gulf of Tonkin. The topography is mainly mountainous terrain that comprises about 70% of the total area at elevations above 500 meters. In the lowlands, elevations range from approximately 0.4 to 9 m, characterized by a tropical climate with summer monsoons from the south and winter monsoons from the northeast (Vinh et al., 2014), the basin experiences average annual precipitation ranging from 800 to 3000 mm. The rainy season occurs from May to October and accounts for 70%-90% of annual rainfall (Quang et al., 2024). Daily rainfall varies from 300-400 mm during this period. The average temperature ranges from 22 to 27 °C, with winter temperatures potentially below 10 °C and summer temperatures above up to 40 °C.

The basin flows into the Gulf of Tonkin through nine river mouths, of which the Tra Ly, Van Uc, and Ba Lat are the main channels for water conveyance. These channels transport a substantial sediment load of approximately 120×10^6

139   tons annually to the Red River Delta region (Vinh et al., 2014). The littoral region has a semi-diurnal tidal regime,

140   with tidal ranges ranging from 2 to 4 m. Saline intrusion significantly influences the littoral region during the dry

141   season with average and maximum wave heights of about 0.7-1.3 m and 3.5-4.5 m, respectively. However, during

142   major storms, wave heights can reach 5 m (Nhuan et al., 2007).

143   The Red River Delta is influenced by several natural hazards, such as flooding, soil salinity, and sea level rise

144   (Castelletti et al., 2012). Several studies have highlighted that rising sea levels are having an increasingly severe

145   impact on inland regions, leading to soil salinity (Nguyễn Văn Đào, 2023). Recently, the Red River Delta in general

146   and the Thai Thuy district in particular have been affected by soil salinity, causing significant damage to agricultural

147   development and negatively impacting residents' livelihoods (Figure 1). According to the FAO report, if the sea level

148   rises by 50 cm, about 11.8% of coastal land is at risk of being flooded by salt water; this figure increases to about

149   31.4% if the sea level rises by 100 cm in Thai Binh province. Recently, saltwater intrusion has clearly affected

150   agricultural production in Thai Binh province and Thai Thuy district. Typically, in the 2015-2016 winter-spring crop,

151   the salinity in the main rivers exceeded the threshold of 1‰, causing significant damage to crops. In 2020, the salinity

152   in the main rivers, 28 km from the sea, exceeded the threshold of 3.75‰, far exceeding the allowable threshold of

153   2.75‰. This phenomenon greatly affects agricultural production in the area.

154

155
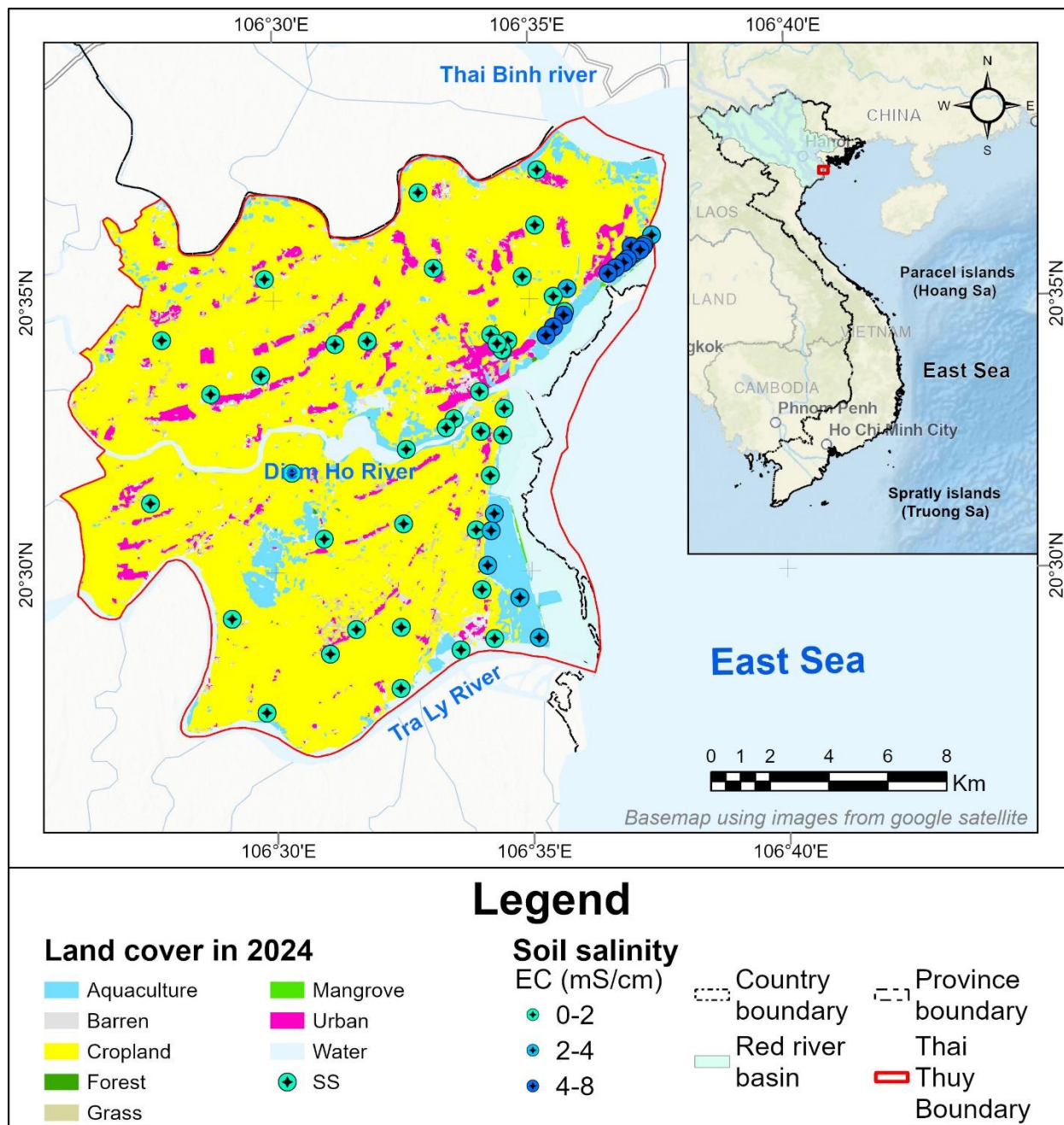
156   Figure 1: Geographical location of study area: The red boundary on the map represents the Thai Thuy district,

157 located in the Thai Binh province in the Red River Delta of Vietnam. The green points are the soil salinity samples

158 collected in April 2024. The land use in the Thai Thuy district is divided into eight types: aquaculture, barren land,

159 cropland, forest, grass, mangrove, urban, and water body. While the aquaculture area is located in the coastal zone,

160   cropland takes up a large part of the study area, and Urban is located in the center and along the road.

161 **3. Methodology**

162 The first strand of the methodology was the identification of the soil salinity mapping. We divided this process into

163 four main steps (Figure 2):

164 Preparation of soil salinity samples and factors

165 The data for constructing the soil salinity map were divided into two main types: EC and conditioning factors.

166 *EC Measurements*

167 We collected soil salinity samples using soil drills, employing both zigzag and grid techniques. Small-scale sampling

168 frequently uses this technique (Elshewy et al., 2024; Jia et al., 2024). The sampling depth depends on the soil salinity

169 assessment for each specific crop. This study monitors soil salinity with the objective of agricultural development;

170 therefore, soil samples were obtained from a depth of 0 to 30 cm. The sampling process occurred in the dry season,

171 between March and April 2024. In addition, when sampling in the field, it is necessary to consider the homogeneity

172 of the soil. We collected 62 samples to cover the entire field. We collected samples along the road to identify different

173 types of soil, and the farmers labeled the samples accordingly. The samples were locked in bags until analysis in the

174 laboratory. We noted the positions of the samples, including longitude and latitude, during the sampling process. When

175 the samples were sent to labs, they were stored in enameled jars, and impurities like stones, wood, and branches were

176 removed. These soil samples were then finely ground. The electrical conductivity (EC) was then calculated from a 1:5

177 soil/deionised water suspension. A soil/water suspension was created by adding 7 g of soil to 35 ml of distilled water

178 and then mixed with a mechanical stirrer for 60 minutes to dissolve the salt. The EC value was measured using a

179 conductivity probe. Finally, the samples were split into two parts: the first part (70%) was used to build the proposed

180 models, while the other part (30%) was applied to confirm the model.

181 *Remote Sensing Data*

182 Due to the effects of the earth's cycle, the salt accumulated in the soil is closely linked to climatic conditions,

183 hydrology, soil characteristics, and surface vegetation density, for example, topographic characteristics (Wang et al.,

184 2024; Xie et al.). We calculated these factors using optical Sentinel 2A images and microwave Sentinel 1 images to

185 determine the soil salinity value. The Sentinel-2A images were calculated by running Sen2Cor for atmospheric

186 correction to ensure the transition between apparent atmospheric reflectance and surface reflectance, and these images

187 were obtained using Google Earth Engine. To reduce the influence of clouds, Sentinel 2A images for March-April

188 2024 were selected with a cloud cover rate of less than 10%. To enhance the quality of these images, the median value

189 of each pixel was calculated at a resolution of 10 m. As for the Sentinel 1 images, they were acquired in dual cross-

190 polarization mode and broadband interferometric mode. The median value of the Sentinel 1 image obtained on March

191 31, 2024, was computed to acquire microwave remote sensing data at a scale of 10 m. As well as 12 bands of the

192 Sentinel 2A image (from band 1 to band 12) and 3 indices of the Sentinel 1 image (VV, VH, and VVVH). In addition,

193 20 spectral indices extracted from Sentinel 2A image were selected to build the soil salinity model, namely Brightness

194 index (BI), Canopy Response Salinity Index (CRSI), Enhanced Vegetation Index (EVI), Intensity index 1 (Int1),

195 Indensity index 2 (Int2), Normalized Difference Salinity Index (NDSI), Normalized Difference Vegetation Index

196 (NDVI), Ratio Vegetation Index (RVI), Salinity index (S1), Salinity index (S2), Salinity index (S3), Salinity index

197 (S5), Salinity index (S6), Soil Adjusted Vegetation Index (SAVI), Salinity Index 1 (SI), Salinity index 2 (SI1), Salinity

198 index 3 (SI2), Salinity index 4 (SI3) and Salinity index 5 (SI4). These factors were divided into three main groups:

199 vegetation indices (NDVI, CRSI, RVI, SAVI, and EVI), water indices (flow direction and distance to river), salinity

200 indices (SI, SI1, SI2, SI3, SI4, S1, S2, S3, S5, S6, and NDSI), topography indices (elevation and slope), and

201 chlorophyll spectral indices (BI, Int1, Int2). These indices have been used frequently in previous studies (Hoa et al.,

202 2019; Nguyen et al., 2021; Wang et al., 2021).

203 The indices due to the vegetation reflect the health and growth of vegetation, and the present study indirectly reflects

204 the level of soil salinity in any region. The increase in soil salinity has a negative effect on the development of

205 vegetation due to the difference in the absorption of water and nutrients; therefore, it leads to a decrease in the values

206 of NDVI, RVI, SAVI, and EVI and an increase in the value of CRSI (Jia et al., 2024; Wang et al., 2024). Water indices

207 play an important role because regions near rivers or along the flow path are more affected by the salinity risk. River

208 flow is often affected by tides or seawater intrusion; therefore, when the distance to the river decreases, the salinity

209 risk increases due to the infiltration of salty river water into the soil. Furthermore, the flow direction influences the

210 propagation and infiltration of water in the soil. Salty water can penetrate further inland if the flow is from the sea to

211 the river, especially in the dry season (Nguyen et al., 2021).

212 Topography indices are key in constructing soil salinity models, as salty water penetrates low-lying regions more

213 easily. In the Red River Delta, the low-lying regions are located along the coastline, and as such, these regions are

214 more affected by the risk of soil salinity. Salinity indices highlight the value of spectral reflectance in regions affected

215 by saltwater intrusion. The higher the salinity, the higher the spectral reflectance value (Du et al., 2024).

216 Construction of hybrid machine learning models

217 We built six machine-learning models to identify the spatial distribution of soil salinity. This involved two main steps:

218 constructing an individual XGB model and then creating hybrid models by integrating each of five optimization

219 algorithms with the XGB model. We developed the XGB model using Python and the Sklearn library.

220 The machine learning model-building process was divided into two main steps: the first was the XGB model building,

221 and the second was the hybrid model building (the integration of XGB with optimization algorithms). The accuracy

222 of the machine learning model depends on the parameter adjustments of the XGB model. In this study, the XGB model

223 parameters were selected using the trial-and-error method. Finally, the XGB parameters were n_estimators=100,

224 max_depth=4, subsample=0.5, and colsample_bytree=0.5. While the hybrid model was built by integrating the XGB

225 model and optimization algorithms, namely GOA, POA, SOA, STO, and PSO. To integrate the XGB model with

226 optimization algorithms, we first need to construct an objective function $F(\theta)$ that returns the error value of XGB on

227 the validation set when using the parameter sets θ. That is, each parameter set has a different error value. Next,

228 determine the search space of the hyperparameters (n_estimators, max_depth, subsample, colsample_bytree) as

229 discrete value intervals. Then, the optimization algorithms will initialize the population of individuals with the size

230 and parameters characteristic of each optimization algorithm. This study was tested with 500 iterations: at each

231 iteration, each individual will generate a combination of θ_i, and the optimization algorithms will update the position

232 or velocity of the individuals according to their own rules. This process is repeated until a stopping threshold is set.

233 Finally, the results are the optimal parameters. The parameters of the model are as follows: problem_size =

234 3, batch_size = 25, epoch = 500, pop_size = 50, "fit_func": fun_avr2, "lb": [0] *problem_size, "ub": [1]* problem_size,

235 c_min = 0.00004, c_max = 2.0 for **XGB-GOA**; problem_size = 3, batch_size = 25, epoch = 500, pop_size = 50,

236 "fit_func": fun_avr2, "lb": [0] *problem_size, "ub": [1]* problem_size, c1=2.05, c2=2.05, w_min=0.4 for **XGB-PSO** ;

237 problem_size = 3, batch_size = 25, epoch = 500, pop_size = 50, "fit_func": fun_avr2, "lb": [0] *problem_size, "ub":*

238 *[1]* problem_size for **XGB-POA**; problem_size = 3, batch_size = 25, epoch = 500, pop_size = 50, "fit_func":

239 fun_avr2, "lb": [0] *problem_size, "ub": [1]* problem_size for **XGB-SOA**; problem_size = 3, batch_size = 25, epoch =

240 500, pop_size = 50, "fit_func": fun_avr2, "lb": [0] *problem_size, "ub": [1]* problem_size for **XGB-STO**.

241 Evaluation of model accuracy

242 The statistical indices, the root mean square error (RMSE), the mean absolute error (MAE), and the correlation

243 coefficient (r) were used to assess the accuracy of the proposed models.

244 Analysis of spatial distribution and identifying the farmers adaptive capacity

245 We validated the models and then used them to assess soil salinity in the study area at a pixel scale with a resolution

246 of 10x10 m. Approximately 30 million pixels were assessed, and a soil salinity map was constructed using the Point

247 to Raster tool in ArcGIS 10.8.

248 We used the second strand of our methodology, interviews with populations, to evaluate the adaptive capacity of farms

249 in the study area. We selected An Tan commune in the Thai Thuy district to participate in structured interviews. A

250 total of 87 households were interviewed. These households were randomly selected from An Tan commune in the

251 Thai Thuy district to participate in structured interviews. The commune is located in the coastal region, which has the

252 lowest altitude and often affected by soil salinity. Residents mainly worked in rice and fish farming. We analyzed all

253 87 responses to assess farmers' ability to adapt to soil salinity.

254 The structured interviews focused on five main elements: natural resources, human resources, physical resources,

255 financial resources, and social resources. There was a particular focus on soil salinity in 2023, allows to evaluate the

256 stress of environment on the livelihood of population.

257

258

259
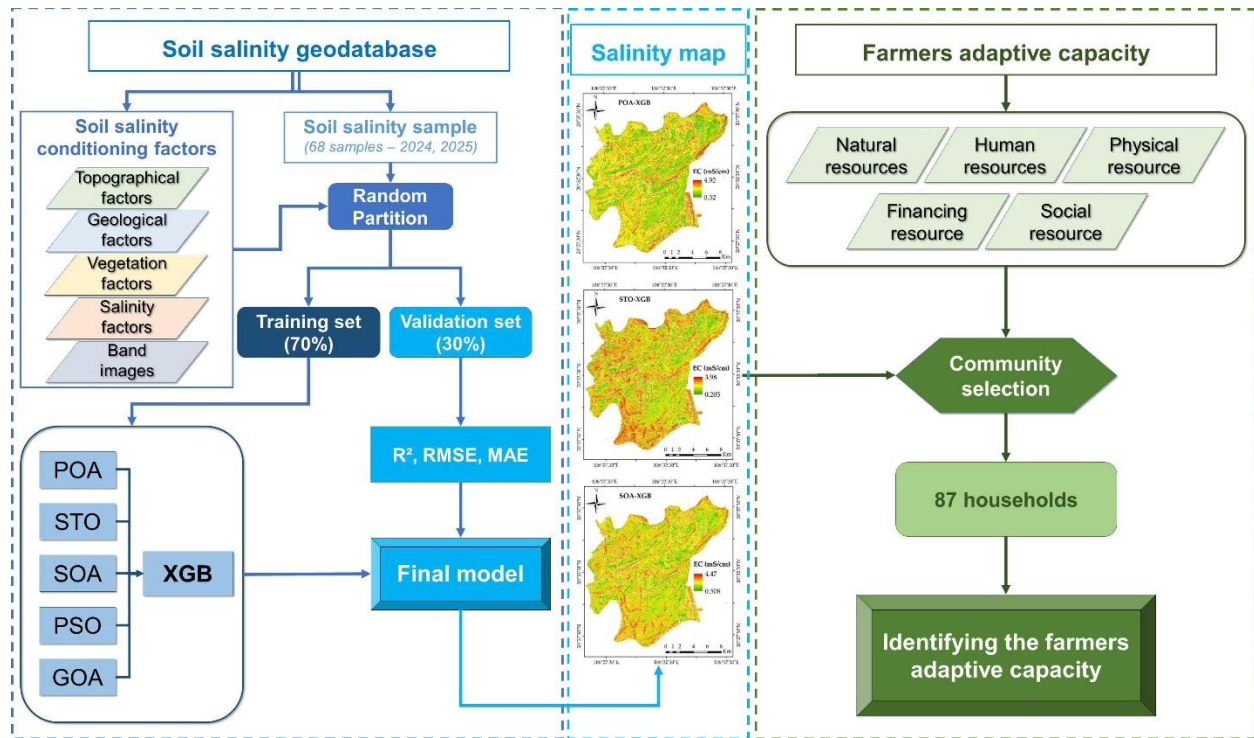
Figure 2: Methodology used for the farmer's adaptive capacity and soil salinity in this study: The methodology used in this study is to design a theoretical framework to assess soil salinity and farmers' adaptive capacity based on machine learning, optimization algorithms, remote sensing, and interviews with local people. We divided this process into four main steps: i) data preparation; ii) machine learning model construction; iii) machine learning model evaluation; and iv) analysis of spatial distribution and identifying the farmers' adaptive capacity.

3.1. XGBoost (XGB)

XGB is a popular gradient-boosted tree algorithm that can solve classification and regression problems. The main idea of learning with XGBoost is to train several models sequentially and combine them successively by correcting errors iteration after iteration to obtain the most potent ensemble model possible (Zhang et al., 2022). Therefore, the prediction result consists of a set of chained decision trees. This method increases the performance and stability of the model while minimizing its variance (Zhang et al., 2022). The XGB model functions in three main steps: i) it constructs an individual model (tree) by taking predictions on the training data, ii) it computes the mistakes of these predictions for the real values, and iii) it constructs another tree to predict and correct these mistakes. The process is repeated, and each new tree is built to correct the mistakes of the previous one. This phase is called "boosting". We then sum up the predictions of all trees to determine the final predictions (Mukhamediev et al., 2023).

276   To optimize the accuracy of the XGB model, three main parameters need to be adjusted: learning rate (reducing the

277   value of this parameter can avoid the overfitting problem), alpha, and lambda (increasing the value of these parameters

278   makes the model more conservative), and column sample by tree (adjusting this parameter has the objective of

279   obtaining the subsample of columns) (Tan et al., 2023).

280   **3.2. Pelican Optimization Algorithm (POA)**

281   Agents searching for prey in nature have a mechanism similar to that of agents searching for optimal solutions.

282   Therefore, based on this perspective, the search agents that comprise a population seek to achieve the optimal solution

283   more quickly. Each agent is an optimal solution whose position is determined in the search space. From a mathematical

284   perspective, agents are vectors, and the population of agents forms matrices (Dehghani and Trojovský, 2022). Among

285   the values used to calculate the aim function, the top value of the agents is determined as the top solution of the agents.

286   One such optimization algorithm is POA proposed by Trojovský and Dehghani (2022). This algorithm is designed

287   based on Pelicans' foraging and communication processes. This is a large bird with a long beak and a large pouch in

288   the throat to hold prey during hunting. Hundreds of individuals may flock together. They can weigh up to 15 kg, grow

289   to a height of 1.8 m, and have a wingspan of up to 3 m. These characteristics greatly assist them in finding food, such

290   as fish, frogs, and turtles.

291   POA is based on the simulation of the behavior and plan of pelicans when attacking prey. Pelican hunting strategies

292   are divided into two stages. First, the bird moves towards its prey, then it spreads its wings and glides along the water

293   surface to attack. In the first stage, the pelicans determine the situation of the prey and move toward the identified

294   prey area. Identifying prey areas represents the determination of the search space in the POA model. The positions of

295   the prey are randomly produced in the search space, which increases the exploration power of POA in the process of

296   searching and solving optimization problems. After locating the prey area in the second stage, pelicans spread their

297   wings and move on the water surface to attack the prey and store it in their throat pouch. This strategy allows them to

298   capture more prey. Modelling this behavior of pelicans makes the POA model easier to converge and improves local

299   search ability (Alamir et al., 2023; Trojovský and Dehghani, 2022).

300   **3.3. Serval Optimization Algorithm (SOA)**

SOA is one of the population-based optimization algorithms, and it exploit the searching power of agents in a population. This property makes this algorithm powerful in solving optimization problems (Dehghani and Trojovský, 2022). Each iteration of SOA continuously determines and updates the agents' situations. The updating process simulates the behavior of serval cats in the wild, divided into two stages: i) exploration of the search space and ii) local exploitation in the search space (Sindi et al., 2024).

Wild cats are some of the most efficient predators, using hearing to identify and attack prey. In the first stage of SOA, the situation of the servals is repeatedly up-to-date after each move: the continuous updating of positions leads to detailed coverage of the search space. The this stage aims is to raise the power to search and explore in the search space. The situation of the best member in the SOA is considered the situation of the prey and, therefore, the optimal solution (Dehghani and Trojovský, 2022; Sindi et al., 2024).

When attacking prey, wild cats jump during the chase to prevent the prey from escaping. These strategies also serve to update the position of the SOA population. The simulation of the chase process can cause small changes in agents' positions in the SOA. However, this phase aims to increase the search space mining capability of SOA, which helps to improve the local search capability in the search space (Dehghani and Trojovský, 2022).

3.4. Siberian Tiger Optimization (STO)

The STO algorithm is a new biologically inspired hyper-heuristic algorithm modeled after Siberian tigers' hunting behavior (Trojovský et al., 2022). STO replicates the Siberian tiger tracking and capture strategy, using a population-based approach to explore the search space efficiently and quickly (Trojovský et al., 2022).

STO works by simulating the way Siberian tigers move and communicate with each other while hunting their prey. Each agent in the STO algorithm represents a Siberian tiger, exploring a different region in the search space. The tigers communicate and share information about their locations with each other to find the optimal location. The location update process of Siberian tigers in STO is carried out in two main phases: the hunting and bear-fighting phases (Trojovský et al., 2022).

In the hunting phase, since the Siberian tiger is a powerful predator, it hunts by attacking different prey, so the agents in the STO are up-to-date based on the simulation of this hunting strategy. After choosing the prey, the Siberian tiger will chase, attack, and kill its prey in this phase. The population continuously updates the members' positions based

327 on the selection and attack of the prey. This phase causes sudden changes in the members' positions and increases the

328 search ability in the search space (Al-Sarray et al., 2024).

329 During hunting, the Siberian tiger has to fight with brown and black bears. Therefore, in the second phase, the members

330 of the STO stay update on the strategies used by the Siberian tiger when bear-fighting. When fighting with bears, the

331 Siberian tiger ambushes and then assaults the bear until it kills it (Al-Sarray et al., 2024; Trojovský et al., 2022).

332 One of the key features of STO is its ability to balance exploration and exploitation. In put it another way, the design

333 of the STO algorithm involves extensive exploration of the search space and refinement of promising solutions in the

334 most promising areas. Thus, STO avoids local optimization problems and increases the likelihood of global

335 optimization (Trojovský et al., 2022).

336 **3.5. Particle Swarm Optimization (PSO)**

337 PSO was proposed by Kennedy and Eberhart (1995). It is founded on the principles of self-organization that allow

338 one or more groups of living organisms to move together in a complex way (Fu et al., 2018). PSO simulates the

339 movement process of some animals, such as flocks of birds. In this model, birds move randomly by following three

340 rules: i) they track the same path as their friends, ii) they are enticed to the average situation of the group, and iii) they

341 maintain a certain space between each other to avoid collisions (Ruidas et al., 2022).

342 PSO explores the search space through the birds' position and flight paths. The position of each bird in the search

343 space is considered a potential solution. More precisely, the position and speed of the birds are represented by vectors

344 with D dimensions, and the initial speed is determined randomly. In the PSO algorithm, the position and velocity of

345 each bird are updated continuously after each iteration until an optimal solution is reached. The optimization function

346 assesses the position and velocity quality (Bui et al., 2016). In this study, PSO was used to optimize the XGB model.

347 **3.6. Grasshopper Optimization Algorithm (GOA)**

348 GOA was first proposed by Mirjalili et al. (2018). This algorithm is based on the swarm behavior of locusts during

349 foraging to solve optimization problems. Grasshoppers move quickly to explore spaces, and then they move locally

350 to exploit resources in the foraging space. GOA models the behavior of a virtual swarm of grasshoppers, where each

351 position represents an optimization solution to the problem (Moayedi et al., 2021; Nguyen, 2022). Movement is

352 influenced by several factors: social interaction, gravity, and wind advection. Social interaction plays an important

353   role in finding the optimal position because grasshoppers interact with each other to exchange information about

354   precise positions. This social communication allows grasshoppers to find the right solutions. Then, gravity allows

355   grasshoppers to explore the foraging spaces in a balanced manner, hence avoiding the local optimization problem

356   (Ingle and Jatoth, 2024). Finally, wind advection represents the external effects that can influence the movement of

357   grasshoppers, leading them to some areas of the search space. In the optimization process, an equilibrium between

358   exploration and exploimportants is important to accurately approach the true global optimum (Moayedi et al., 2020).

359   **4. Results**

360   **4.1. Soil Salinity Predictors**

361   The choice of suitable factors plays a key role when using machine learning to determine the geographical distribution

362   of soil salinity in any region. Conditioning factors represent the causes of soil salinity, so improper selection of these

363   factors can result in inaccurate prediction. Data redundancy may complicate the model and lead to poor performance.

364   In this study, we used RF to measure the appropriate factors. It assigns a value to each factor based on its relationship

365   with the soil salinity samples and the conditioning factors. The most important factor is the one with the greatest

366   importance in determining soil salinity zones. In addition, after using RF to determine the importance of factors, we

367   used trial and error to continue eliminating factors that affected the precision of the model.

368   The outcome showed that six factors (DEM, RVI, B2, S6, S2, and S1) had an RF value of zero, so these factors did

369   not affect the determination of the spatial distribution of saline areas. In addition, two factors (NDVI and flow

370   accumulation) were eliminated using the trial-and-error method. The other 30 factors were used to build the model.

371   VVVH (0.39), VV (0.3), distance from the river (0.28), CRSI (0.24), and EVI (0.21) had a strong influence on the soil

372   salinity in the study area. S3 (0.17), BI (0.17), B12 (0.15), SI2 (0.14), B7 (0.11), VH (0.1), and Int2 (0.1) have moderate

373   relationships with the soil salinity. B11 (0.08), S5 (0.06), slope (0.06), SI (0.06), SAVI (0.06), NDSI (0.06), SI4 0.05),

374   B5 (0.05), Int1 (0.05), B9 (0.05), B4 (0.05), SI (0.04), SI1 (0.04), B8 (0.04), B3 (0.02), B1 (0.02), and B6 (0.02) had

375   only a weak relationship on soil salinity (Figure 3).
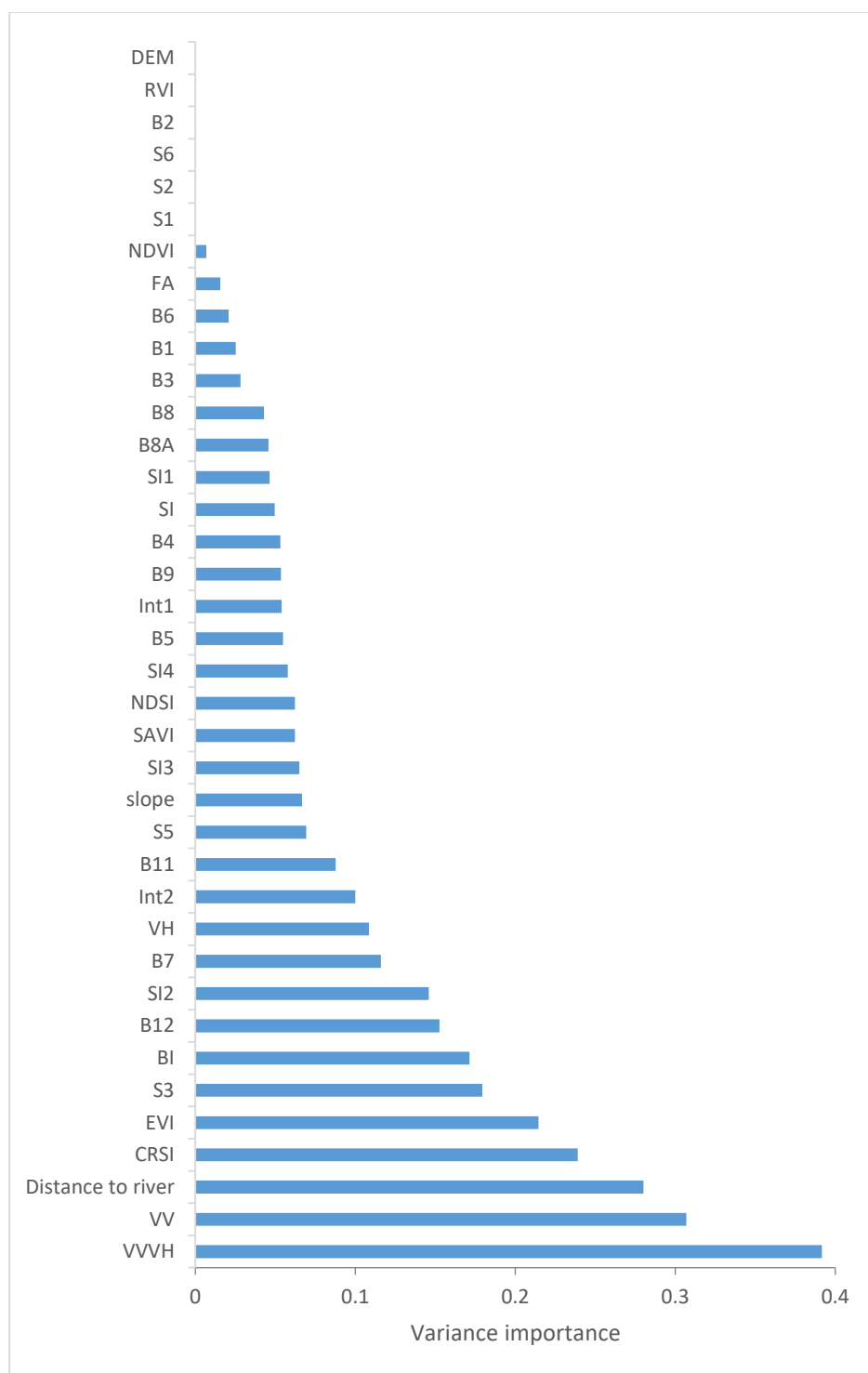
Figure 3: Variables important for soil salinity model using RF.

380 **4.2. Model Accuracy Validation**

381 R^2 was used to assess the performance of the machine learning models. The outcome of this study demonstrated that

382 all optimization algorithms enhanced the performance of the XGB model. The XGB-POA model was the greatest,

383 with an R^2 value of 0.968, followed by XGB-STO (R^2=0.967), XGB-SOA (R^2=0.966), XGB-PSO (R2 = 0.964), and

384 XGB-GOA (R^2=0.964; Figure 4).
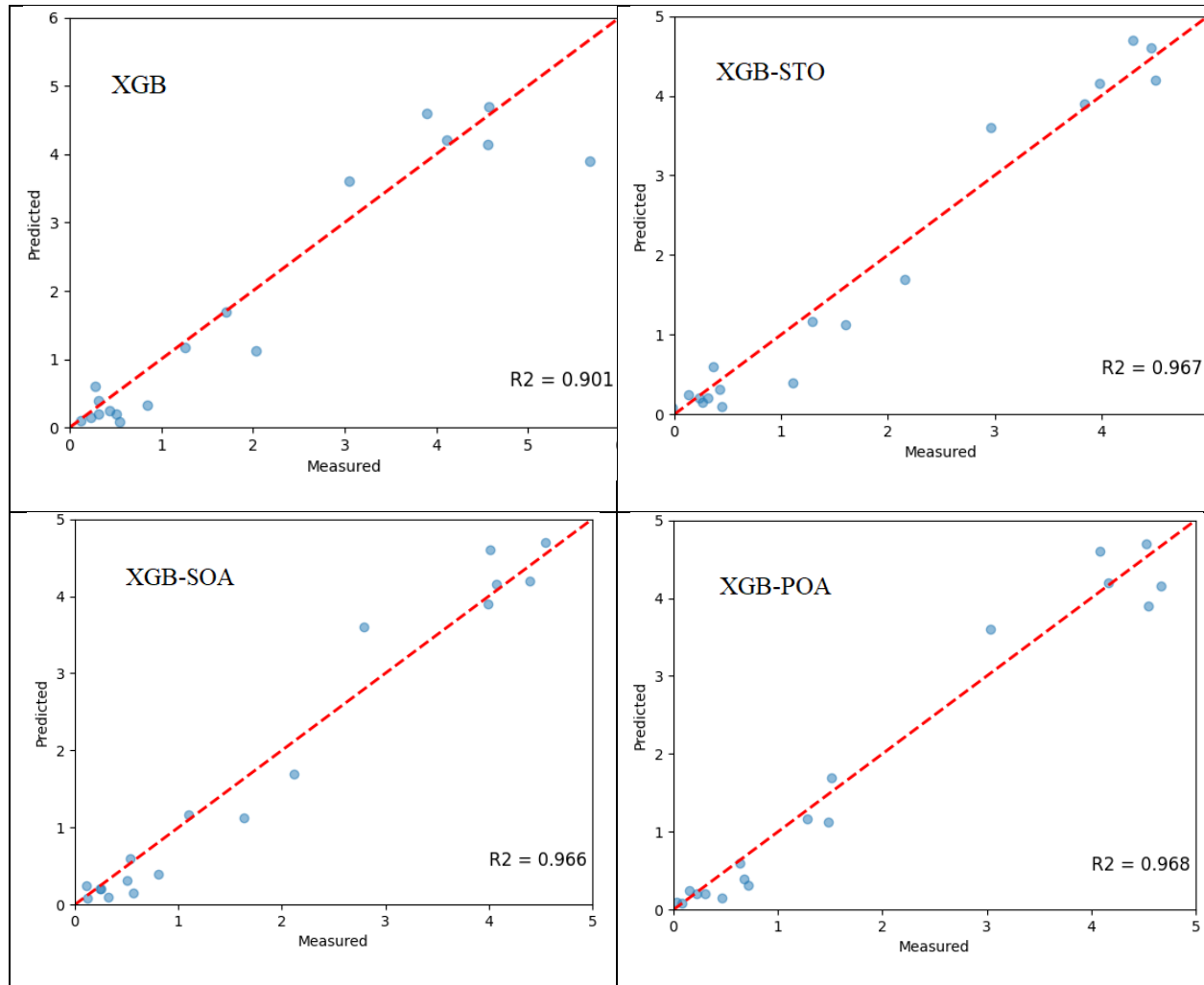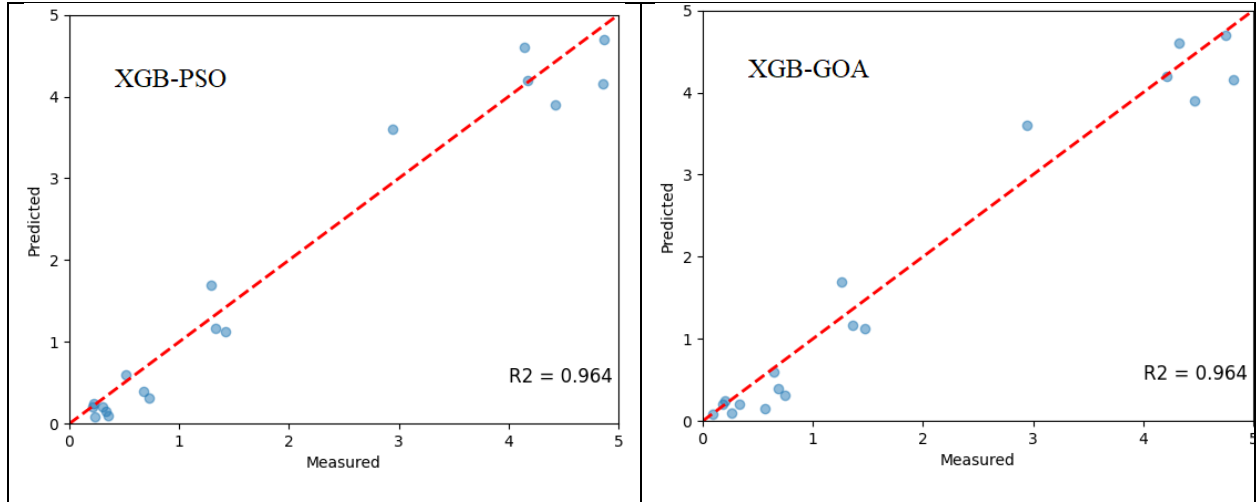
Figure 4: R² value for the testing dataset

The RMSE and MAE were also used to evaluate the accuracy of the machine learning models. The XGB-POA model performed better on training and validation data (RMSE=0.28, MAE=0.18 for learning data and RMSE=0.31 and MAE=0.242 for verification data). The XGB-STO was ranked second with an RMSE value of 0.3 and MAE of 0.22 for learning data, and an RMSE value of 0.32 and MAE of 0.244 for verification data. The XGB-SOA model was ranked third, with RMSE=0.31 and MAE=0.23 for learning data and RMSE=0.33 and MAE=0.25 for verification data. XGB-GOA model came fourth, with RMSE=0.33 and MAE=0.25 for learning data and RMSE=0.34 and MAE=0.26 for verification data. The XGB-PSO model performed less well than the other models, with RMSE=0.335 and MAE=0.26 for learning data and RMSE=0.341 and MAE=0.27 for verification data (Table 1).

Table 1. Model performance and comparison.

Models	Training dataset			Validation dataset		
	RMSE	**MAE**	**R²**	**RMSE**	**MAE**	**R²**
XGB-POA	0.28	0.18	0.99	0.31	0.242	0.968
XGB-STO	0.3	0.22	0.987	0.32	0.244	0.967
XGB-SOA	0.31	0.23	0.98	0.33	0.25	0.966
XGB-GOA	0.33	0.25	0.97	0.34	0.26	0.964
XGB-PSO	0.335	0.26	0.97	0.341	0.27	0.964
XGB	0.35	0.32	0.91	0.37	0.34	0.901

4.3. Spatial distribution of soil salinity in the Thai Thuy district of the Red River Delta

Following validation, we constructed a geographical distribution map of soil salinity using the proposed models. We carried out the process by assigning conditioning factors to the 30 million pixels across the entire study area. Depending on each model, the EC value varies from 0.29 to 7.7 mS/cm. On the map, the color varies from green to red, representing different EC values. The areas with green colors are located far from the continent (EC = 0.29), while the areas with red colors are located on the coast, with EC values superior to 7.7 mS/cm. This graph shows that these areas are directly affected by saltwater intrusion from the sea (Figure 5).

According to the FAO, salinity can be divided into 5 levels: non-saline, slightly saline, moderately saline, heavily saline, and very heavily saline. In which the EC value is below 2 mS/cm, the soil is considered not saline, and the plants grow completely normally. The EC value ranges from 2- 4 mS/cm; the soil is slightly saline and has very little effect on the plants. Specifically, flower crops may grow slowly, while rice and fruit trees may have reduced height. The EC value ranges from 4-8 mS/cm; the soil is moderately saline and reduces crop yields. Specifically, rice can have a 10-20% reduction in yield. The EC value ranges from 8 - 16 mS/cm; the soil is heavily saline and affects the growth of plants. The soil becomes extremely saline and uncultivated if the EC value surpasses the threshold of 16 mS/cm. This study utilizes the XGB-POA model, which boasts the highest accuracy, to analyze the areas affected by saline intrusion. Specifically, in the study area, about 65 km² of land area is not affected by saline intrusion, 165 km² is slightly affected, and 1.8 km² is greatly affected by saline intrusion. Compared to the land cover/land use map, it can be seen that the land area greatly affected by saline intrusion is mainly aquaculture; therefore, this area will not be significantly affected in terms of productivity. Meanwhile, 165 km2 of land affected by saline intrusion is rice land, which can slow down rice growth and reduce productivity.

In the study area of Thai Thuy District, Thai Binh Province, about 70-75% of the agricultural land is irrigated by a canal system that draws water from the Red River and the Day River. Thanks to the water source from the Red River and the Day River, agricultural production areas are regularly washed away with salt, so the EC value in these areas is often below 4 mS/cm. In coastal areas, salinity intrusion at river mouths forces people to use shallow groundwater for irrigation, which leads to salt accumulation and prompts a shift from rice cultivation to aquaculture.
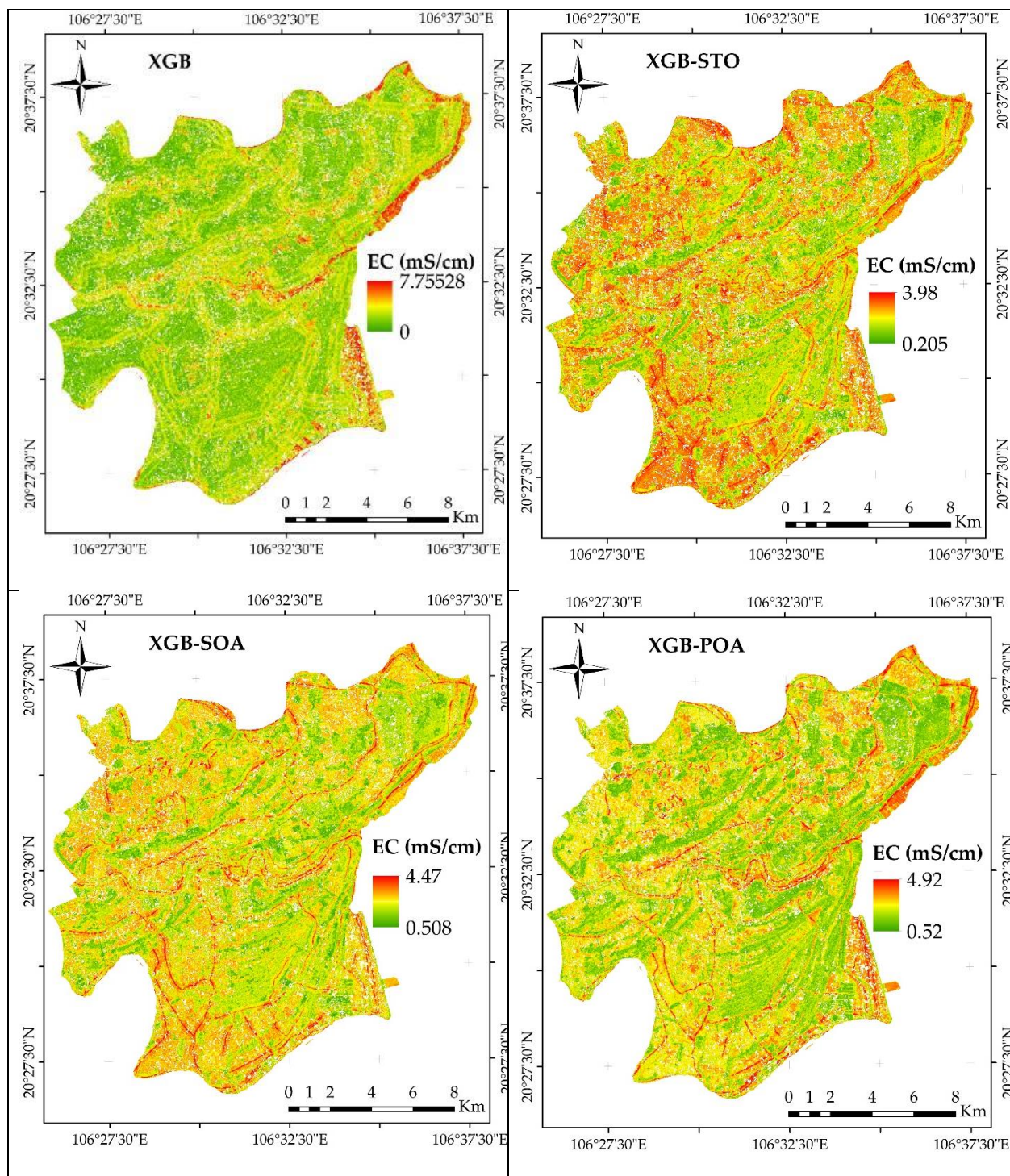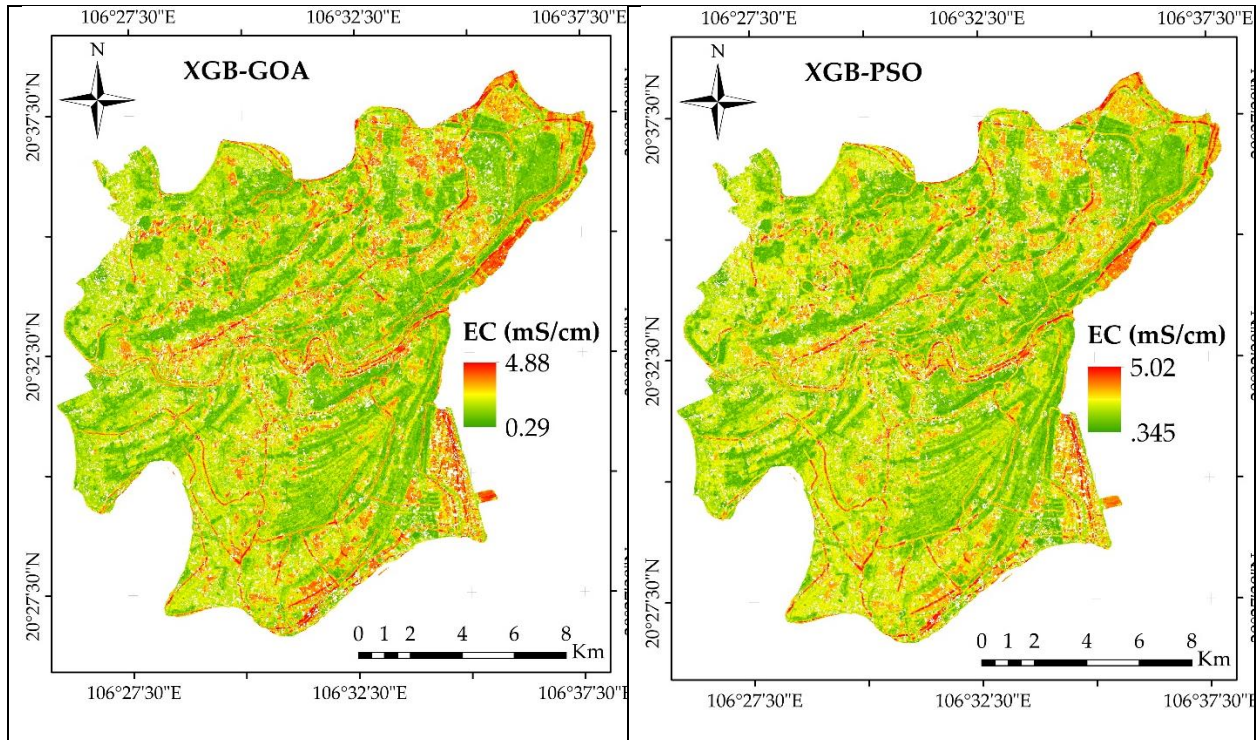
Figure 5: Soil salinity mapping in the Thai Thuy district

4.4. Farmers' Adaptive Capacity Assessment

Soil salinity is a key challenge for deltas worldwide, particularly in deltas where population density is high and socio-economic conditions are poor (Hoque et al., 2016). The Red River Delta is the most densely populated area in Vietnam and one of the most densely populated deltas in Southeast Asia; therefore it is crucial to consider the impact of soil salinity in this delta on the farmer's life and their adaptive capacity. Spatial distribution maps of soil salinity show that this phenomenon occurs in many areas of the Thai Thuy district, especially in coastal areas. This phenomenon certainly has a significant impact on people's living conditions and production areas, posing challenges to their livelihoods. In this section, we address the adaptive capacity of farmers in An Tan commune, a coastal area, through five elements: i) natural resources including land use, awareness of saline intrusion, perceived impacts on agricultural activities, and adaptation measures taken, ii) human resources such as household demographics, education, and farming experience, iii) physical resources, including the availability of farming equipment and infrastructure, iv) financial resources focusing on household income, income structure, credit access, and changes over time, and v) social resources addressing support from government and social networks, community cooperation, and participation in collective

435   adaptation activities. We interviewed 87 households in the An Tan commune to analyze the community's ability to

436   adapt to saline intrusion.

437   *4.4.1. Natural Resources*

438   Due to the process of salinization, we are facing a major threat to agriculture and sustaining arable land. Excess salinity

439   adversely influences soil structure and fertility, plant growth, crop yield, and microorganisms (Tarolli et al., 2024).

440   Soil salinity is frequently associated with water salinity. Groundwater in littoral regions of the Red River Delta is

441   characterized by high salinity (Hoque et al., 2016). The scarcity of freshwater poses significant challenges for crop

442   irrigation. Irrigating with saline water exacerbates soil salinity. In addition, soil salinity also creates a scarcity of

443   grazing land and fodder cropland of coastal areas. Coastal livestock is harshly suffering from food inaccessibility and

444   poultry farming in the coastal districts. All the mentioned factors impose considerable risks to the coastal inhabitant's

445   livelihood and food security, who rely mainly on agricultural activities such as growing rice and crops such as onions,

446   garlic, watermelon, and tobacco, according to our interviews.

447   Indeed, the results showed that 59% of interviewed households said that salinization had a medium to high impact on

448   agricultural production in the area in recent years, especially during the 2023 saline intrusion. Meanwhile, 38% of

449   households stated that saline intrusion has little or very little impact on agricultural production, mainly households in

450   areas far from the coast and so less affected. Households in the study area have implemented various measures to

451   mitigate the increasingly serious saline intrusion, such as washing the salt from the fields after each crop (as instructed

452   by local authorities) and adjusting their cropping systems by adopting salt-tolerant crop varieties or transitioning to

453   aquaculture practices. 66% of interviewed households said they had to change the crop structure to suit the saline

454   intrusion or switch to non-agricultural occupations to earn more income. Of the 87 households interviewed, 28% had

455   their main income from non-agricultural activities. A large number of people switching to non-agricultural activities

456   can meet their livelihood needs, but in the long-term, farmers abandoning agricultural activities to seek jobs in factories

457   or migrate to cities also poses many negative environmental and social consequences, such as the decline of

458   agrobiodiversity or labor shortages in agriculture, etc. (Subedi et al., 2022).

459   *4.4.2. Human Resources*

460 In agricultural production and the adaptability of the community to salinity intrusion, demographics are considered

461 one of the most important factors contributing to the creation of labour resources, directly affecting crop productivity.

462 The results of interviews with 87 households showed that each household has an average of 3.5 members, comprising

463 2.5 workers and 1 dependent member. Using available family resources reduces labor costs, thereby increasing

464 production profits. However, the quality of human resources poses a concern when adapting to saline intrusion. One

465 of the criteria for evaluation is education level. Most workers in households had a junior high school degree (66%),

466 5% of interviewees had a high school degree, and less than 3% had a university degree. According to previous studies,

467 education is an important factor in determining workers' income. In the context of climate change and sea level rise,

468 agriculture is negatively affected by these phenomena: low levels of education mean a lesser ability to absorb new

469 knowledge and methods in organizing production to reduce the negative impacts of saline intrusion. Although 83%

470 of the interviewed households had more than 20 years of experience in agricultural production, their knowledge of

471 saline intrusion and climate change was still limited. Specifically, people lack the adequate knowledge and skills to

472 adapt to changes in environmental conditions, leading to difficulties in choosing appropriate livelihood models.

473 Furthermore, saline intrusion has led to several health insecurity. Coastal residents in saline areas are at risk of

474 consuming high salt above the recommended levels. It is evaluated that over 7 million coastal populations in

475 Bangladesh, India, and Vietnam suffer from hypertension and cardiovascular diseases as a result of long-term

476 ingestion of saline groundwater (Hoque et al., 2016). This has profound consequences for the development and quality

477 of human resources in these areas.

478 *4.4.3. Physical Resources*

479 Material resources include essential items that serve people's daily life and livelihoods. The majority of the households

480 interviewed were engaged in agriculture, so the means of production were mainly related to agricultural activities. Of

481 the 87 households interviewed, 90% were equipped with agricultural production equipment such as pumps, sprayers,

482 and tractors, while 100% had access to tractors and harvesters for farming. The interviewed households used

483 equipment to exploit water sources for agricultural production; however, because the town of An Tan is located in a

484 coastal area, groundwater and surface water are often affected by saline intrusion. Thus, they still faced challenges

485 related to water resources, especially in the context of saline intrusion

486 Moreover, in response to saline intrusion, accessing freshwater for daily use and irrigation often leads to the

487 spontaneous extraction of groundwater through tubewells, a common practice in coastal areas of Vietnam and

488 Southeast Asia (Hoque et al., 2016). However, excessive groundwater extraction and improper irrigation practices

489 also pose many potential risks of increasing water resource depletion and accelerating salinization processes (Tarolli

490 et al., 2024). This will likely undermine the long-term adaptive capacity of coastal communities.

491 *4.4.4. Financial Resources*

492 The interviews with 87 households demonstrated that 9% of the households interviewed were poor and near-poor. It

493 can be seen that economic status greatly affects people's ability to adapt and recover from soil salinity. Poor and near-

494 poor households frequently have more difficulty evaluating solutions to mitigate the impact of soil salinity on

495 agricultural production. The primary source of income for a large part of the population mainly comes from

496 agricultural activities: 72% of the households interviewed confirmed that their main livelihood was agriculture.

497 However, their agricultural income is frequently unstable. This stresses the vulnerability of people's livelihoods due

498 to the strong effects of soil salinity on agricultural activities. Meanwhile, 56% had a stable source of income from

499 factory work. This emphasizes the need to diversify income sources for inhabitants in soil salinity areas. In addition,

500 although the income from agricultural production was enough to cover farmers' daily life, most of the households

501 interviewed could not save. Therefore, with increasing saline intrusion in the context of climate change, it is very

502 difficult for these households to have an effective response or adaptation solutions. Borrowing capital to overcome

503 the negative impacts of saline intrusion is one of the adaptation strategies reported by the interviewed households.

504 36% of households borrowed capital from relatives, 11% borrowed from credit funds or banks, 14% from local

505 organisations, and 33% from distribution agents. Meanwhile, 8% of the interviewed households could not borrow any

506 capital to overcome the consequences of saline intrusion.

507 Diversifying external sources of capital can help households overcome the consequences of saline intrusion and

508 support agricultural production more generally. However, there are still several people who cannot access capital

509 sources, and training to the adaptability and resilience of the people. This increases the impact of soil salinity on the

510 community in the study area. Furthermore, a capital utilization strategy must be carefully considered to ensure efficient

511 use of resources to improve livelihoods and enhance adaptability to saline intrusion.

512 4.4.5. *Social Resources*

513 Social resources play a key role in mitigating the impacts of soil salinity on the adaptability and resilience of the

514 people. In the study area, households received support from various sources, such as local communities, volunteer

515 organizations, non-governmental organizations, and mutual assistance among households. This support includes

516 exemption from land use tax, support for production equipment, crops, and food supply for people. Regarding people's

517 awareness of climate change and its impact on salinity intrusion, about 82% of households said they learned about

518 this issue through local authorities and media propaganda.. Furthermore, 100% of the households surveyed reported

519 that local authorities also had organised training sessions and drills to respond to saline intrusion and sea level rise.

520 However, as mentioned above, the knowledge and skills of inhabitants are still limited. This raises questions about

521 the effectiveness of training sessions. In addition, these training activities occur infrequently. For example, during the

522 soil salinity, people did not receive timely support and assistance from these organisations. This led to a reduction in

523 the community's ability to adapt soil salinity.

524 **5. Discussion**

525 Soil salinity is a global environmental threat, a key cause of food insecurity worldwide (Song et al., 2024). Therefore,

526 it is essential to monitor it with high precision, as is identifying the adaptive capacity of those in vulnerable regions.

527 In Vietnam, two large deltas ensure food security not only, but also in other countries. Although several previous

528 studies have been conducted to assess soil salinity in Vietnam, most have focused on assessing soil salinity and

529 farmers' adaptive capacity in the Mekong Delta (Hoang and Hai, 2024; Nguyen et al., 2024). Research on the Red

530 River Delta is scarce. The Red River Delta is one of the key agricultural regions in Southeast Asia. Therefore, assessing

531 soil salinity and farms' adaptive capacity in this area is necessary. In this study, remote sensing, machine learning,

532 and community interviews were used to evaluate soil salinity and the adaptive capacity of farms in the delta.

533 Remote sensing plays a key role in analyzing soil salinity because the salt in the soil has a significant effect on the

534 spectral reflectance of the soil. Soils with different salinity levels will have different spectral characteristics; for

535 example, areas covered with white salt often have higher spectral reflectance levels and salinity (Hoa et al., 2019; Wu

536 et al., 2018; Xiao et al., 2023). This is the basis for using remote sensors to monitor saltwater intrusion. However, one

537 of the challenges in using Sentinel 2 satellite images in soil salinity monitoring is that sometimes, the spectral

538 reflectance level is not consistent with soil salinity. Many studies have integrated vegetation indices in soil salinity

539 monitoring to minimize this limitation because different areas will have different soil salinity. It should also be noted

540   that the difference depends on the vegetation type in each area. Therefore, this study has integrated Sentinel 1 images

541   in soil salinity monitoring. Sentinel 1 images use radar signals to monitor moisture and dielectric properties providing

542   accurate information on soil salinity. This is particularly important in coastal areas, where surface moisture is high,

543   reducing the accuracy of optical imagery. This approach identifies areas severely affected by salinity intrusion while

544   supporting the assessment of the adaptive capacity of communities in the area (Hoa et al., 2019). However, with the

545   increase in the volume, type, and speed of remote sensing data collection, bottlenecks in the data analysis process may

546   occur (due to the inadequacy of the structure of current models for processing large datasets).

547   XGB is one of the most powerful algorithms for identifying the spatial distribution of natural hazards, such as floods,

548   landslides, and soil salinity. Its advantages include the ability to avoid the overfitting problem and fast convergence.

549   Additionally, XGB effectively handles missing values (Liu et al., 2022; Mo et al., 2019). However, both the

550   configuration and interpretation of XGB are more complex, and the parameters of this model are also complex to tune.

551   Incorrect parameter selection can reduce performance (Ramraj et al., 2016). Therefore, it is necessary to use

552   optimization algorithms to select the parameters of this model. In this study, five optimization algorithms, namely

553   POA, STO, SOA, PSO, and GOA, were utilized to optimize the parameters of XGB. The XGB-POA model

554   outperformed the other models as it is easy to carry out, has few parameters to adjust, has faster convergence capability,

555   and can avoid local minima - which enables it to find the best global solution (Premkumar and Santhosh, 2024).

556   Previous studies have indicated that POA also can solve complex problems with a large number of variables and non-

557   linear properties (Alamir et al., 2023; Li et al., 2023). XGB-STO model ranked second. The STO algorithm maintains

558   a good equilibrium with exploration and exploitation processes. This allows it to avoid local minima problems, which

559   improves model performance (Al-Sarray et al., 2024; Trojovský et al., 2022). The XGB-SOA model came third in

560   terms of accuracy. SOA can solve complex problems with a large number of variables or continuous, discrete, or

561   multi-objective problems, so it is a versatile tool for several different applications. In addition, inspired by the serval's

562   precise jumps and fast movements, SOA can converge quickly with high accuracy (Dehghani and Trojovský, 2022;

563   Sindi et al., 2024). The XGB-PSO model was ranked fourth. In addition to ease of use, PSO has the advantage of

564   equilibrium of the exploration and exploitation processes. This can avoid the local optimization problem (Juneja and

565   Nagar, 2016; Rini et al., 2011). The XGB-GOA model was less accurate than other models because it tends to

566   concentrate exploration at the beginning of the process to avoid the local optimization problem. This may lead to slow

567   convergence (Mirjalili et al., 2018; Zhao et al., 2019). When comparing the models proposed in this study on the

568   ability to predict natural hazards such as soil salinity, each model has different characteristics that influence the real-

569   time prediction ability. Three models (XGB-POA, XGB-STO, and XGB-SOA) can converge quickly because of the

570   faster learning speed. Therefore, these models best suit adaptation for real-time applications because fast updates are

571   necessary to support those tasked with developing mitigation strategies.

572   The results of this study not only confirmed the effectiveness of XGBoost models in soil salinity prediction but also

573   showed the potential for improving accuracy by combining them with optimization algorithms. Compared with

574   previous studies, the models in this study outperform traditional models. Wang and Sun (2024) used three machine

575   learning models, namely random forest (RF), support vector machine (SVM), and artificial neural network (ANN), to

576   predict the soil salinity in Huludao City, China. The results indicated that the RF model performed better with an R^2

577   value of 0.84. The model accuracy in Wang and Sun's 2024 study was lower than the models in our study. Aksoy et

578   al. (2024) applied two models, namely XGB and RF to predict the soil salinity in western and southeastern Lake Urmia

579   Playas (LUP) in the Northwest of Iran. The results showed that the XGB model was more efficient with the R^2 value

580   of 0.83. It was less accurate than in our study. Elshewy et al. (2024) evaluated the soil salinity in Sharkia Governorate,

581   Egypt, using four machine learning models, namely support vector machines (SVM), regression trees, Gaussian linear

582   regression, and tree-based ensemble. The results indicated that the SVM model performed better with an R^2 value of

583   0.86. Comparison with previous studies showed the potential of the machine learning model in this study to predict

584   soil salinity.

585   Saline intrusion in the Red River Delta and the study area reflects the interaction between natural factors and human

586   activities. One cause of the increasingly serious saline intrusion in the study area is the reduced flow in the delta caused

587   by the construction of dams and reservoirs upstream in China. This reduction reduces the ability of the river system

588   to repel salt water, creating conditions for seawater to penetrate deep into the inland. Hien et al. (2023) have

589   emphasized that by 2050, saltwater intrusion is likely to extend about 20 km inland from the river mouth, related to

590   sea level rise and reduced discharge from the upper river. Nguyen et al. (2017) reported that the increasing trend of

591   saline intrusion is the result of sea level rise, combined with the decline of the Red River water level, especially in the

592   dry season. Specifically, the sea level increased by 0.19 m in the period 1901-2010, with an average rate of 3.2 m from

593   1993-2010. In addition, the phenomenon of saline intrusion is increasingly severe due to subsidence related to

594   groundwater exploitation. In many areas of the Red River Delta in general and the study area in particular, uncontrolled

595 groundwater exploitation for agricultural production and aquaculture contributes to subsidence, increasing the impact

596 of tides. Nguyen and Takewaka (2020) have emphasized that the subsidence phenomenon in the delta can reach -12.3

597 mm/year, which is one of the causes that aggravate the problem of saltwater intrusion, especially in the context of

598 rising sea levels.

599 The results of this study explored the adaptive capacity of farms in the Thai Thuy district of Thai Binh province.

600 Riverine farmers in areas affected by saltwater intrusion are prepared. They rely on their local communities and expect

601 support from local authorities and voluntary organisations. Our results are similar to those of previous studies

602 investigating the adaptive capacity of residential communities to natural hazards, including saltwater intrusion. The

603 key to adaptation is education, knowledge, and resources to cope with saltwater intrusion. These resources can be

604 natural, physical, financial, social, and human resources.

605 The community's adaptive capacity in the study area faces many challenges, especially in the context of global

606 warming and growing saltwater intrusion. Although most households surveyed have more than 20 years of experience

607 in agricultural production and benefit from available labor resources, their adaptive capacity to saltwater intrusion

608 remains limited. This is in part because these households lack the knowledge to change their livelihood patterns in

609 addressing varying environmental situations. In addition, the main sources of agricultural income are often unstable,

610 and the ability to accumulate finances is low, leading to difficulties in adapting to and recovering from saltwater

611 intrusion. People's adaptation strategies, such as uncontrolled groundwater extraction and conversion to non-

612 agricultural activities, also present long-term environmental and social risks. Furthermore, policies and support

613 programs for residents, such as training sessions and lending programs provided by stakeholders, also raise concerns

614 regarding their effectiveness and inclusiveness. Although people in the study area have access to capital from many

615 different sources, some households still cannot access these sources of capital to overcome the consequences of

616 saltwater intrusion. All of these factors impact agriculture and human life, leading to increased household

617 vulnerability. To enhance people's adaptive capacity, it is important to emphasize the role and effectiveness of policies

618 of local governments, policymakers and stakeholders in supporting people to understand better and respond to saline

619 intrusion. Information and knowledge sharing can be done through direct outreach to people to raise awareness of

620 saline intrusion among communities. Lending policies of local governments and stakeholders need to cover all

621 households while improving the efficiency of capital use. Effective management of natural and physical resources and

622 enhancing social capital through the development of cooperative community models are important factors contributing

623 to people's adaptive capacity to saline intrusion. This study has successfully built a theoretical framework using

624 machine learning with optimization algorithms, remote sensing, and farmer interviews to determine the spatial

625 distribution of soil salinity and farmers' adaptation capacity. However, to apply this theoretical framework in different

626 regions, it is necessary to use factors specifically pertinent to each region. Machine learning models must be provided

627 with the local characteristics of the region in question. However, data collection in any region is difficult, often due to

628 restrictive data-sharing policies or limited financing resources to maintain and distribute the data.

629 From field surveys, it can be seen that in the Red River Delta, adaptation options to soil salinity mainly rely on

630 upgrading the sea dike system, river dikes, and saline prevention sluice systems. In addition, other adaptation options

631 mainly include increasing the resilience of the current agricultural system, such as changing the crop calendar,

632 changing crop varieties, using fertilizers, and planting mangroves. Many households have transitioned from rice

633 cultivation to aquaculture in coastal areas, where soil salinity has a significant impact. In addition, some fish farming

634 households have also switched to shrimp farming or fish farming due to increased saline intrusion. Some households

635 do not have the capital to convert their agricultural systems, and while agricultural productivity decreases due to saline

636 intrusion, they consider finding non-agricultural jobs or migrating to the city to find jobs with more stable incomes.

637 Households located further inland, less affected by saline intrusion, still maintain traditional agriculture. Some

638 households practice intercropping by growing rice alongside vegetables to increase their income. Thus, it can be seen

639 that the adaptability of households in the Red River Delta is not only based on strengthening the system of sea dikes,

640 river dikes, and salinity prevention sluices, but also on transforming the traditional agricultural system to minimize

641 the impact of salinity intrusion. However, capital barriers force many households to abandon agriculture, seriously

642 affecting the food security situation in the region.

643 A significant problem when using machine learning is that of extrapolation. Each model built is adapted only to one

644 set of data. Therefore, evaluating the soil salinity in other regions is challenging. General, there is only one model

645 that fits each training dataset. In theory, this would not be a problem if enough training data were collected and all

646 extreme events were included. However, in practice, it is very difficult to collect data for all these events, especially

647 in the context of climate change and sea level rise.. To solve this problem, several studies have pointed out that

648 integrating machine learning with conventional models for example, remote sensing or hydrodynamic models can be

649   effective, as such traditional models can provide the training data to use as the input file of the machine learning

650   model. Another solution is to combine machine learning with optimization algorithms, as in this study, to enhance the

651   prediction capability of the machine learning model (Tran and Kim, 2022).

652   This study emphasizes the significance of combining machine learning methods to analyze the spatial distribution of

653   salinity intrusion with the community's adaptive capacity to soil salinity. The salinity intrusion map from the machine

654   learning model shows a clear difference in the level of salinity intrusion between coastal, riverside, and inland areas.s.

655   Coastal and estuarine areas often have high levels of salinity intrusion, with EC values exceeding 7 mS/cm. These are

656   also areas where communities must apply appropriate adaptation strategies, including crop restructuring, selecting

657   more salinity-tolerant plant varieties, combining agriculture and fisheries, or livelihood conversion. In contrast, inland

658   areas, where the level of salinity intrusion is lower, have less variation in agricultural production models, and

659   communities in these areas still mainly maintain traditional agricultural practices. The findings may indicate that the

660   coping strategies and adaptive capacity of the communities depend on the level of salinity intrusion in the areas. In

661   addition, it can be seen that in areas with high salinity intrusion, people have difficulty in accessing fresh water for

662   agricultural production; therefore, the communities in this area tend to depend more on non-agricultural sources of

663   income. Previous studies (Nguyen et al., 2019; Yuen et al., 2021) have demonstrated this trend.

664   The results of the study emphasize that the integration of advanced machine learning models and sociological surveys

665   not only improves the comprehensive research ability from natural factors to socio-economic factors but can also

666   support policymakers and planners to develop appropriate adaptation solutions. Identifying areas affected by saline

667   intrusion by using machine learning models and qualitative analysis of the adaptive capacity of the community is a

668   solid scientific basis for developing policies to minimize the impact of saline intrusion, especially in the context of

669   climate change, to ensure agricultural development and food security.

670   This study was successful in building machine learning models integrated with optimization algorithms to identify the

671   spatial of soil salinity, as well as evaluating farmers' adaptive capacity in the study area. However, in terms of data,

672   this study collected 62 soil salinity samples to build the machine learning model; therefore, the soil salinity map

673   constructed by the proposed models cannot present the trend and drive of soil salinity in time series. Furthermore, soil

674   salinity is significantly affected by climate change and rising sea levels, so it is necessary to assess the effects of this

675   change on soil salinity in the future.

676 As hydrological conditions change, those living in deltas are confronting increased risk. The Red River Delta is one

677 of the largest deltas in the world and, thanks to its fertile floodplains, is home to about 21 million inhabitants. In recent

678 years, in the context of global warming and rising sea levels, these deltas are confronting growing flooding and soil

679 salinity problems, which affect food security in the region and the country. Policies must be implemented to improve

680 the agricultural system and the adaptive capacity of farmers. A proactive approach is required, envisaging multiple

681 scenarios to provide appropriate support for agriculture. These scenarios may include activities and programs adaptive

682 to the different influences of global warming on soil salinity.

683 **6. Conclusion**

684 Soil salinity is a key environmental threat, which will have a growing effect on the development of agriculture and

685 food security globally. A lack of assessment of local adaptive capacities exacerbates the problem. Therefore, this

686 research's objective was toconstruct a theoretical framework to assess soil salinity and farmers' adaptive capacity

687 based on machine learning, optimization algorithms, remote sensing, and interviews with local people. The results in

688 this study represent a novel contribution to the literature for researchers worldwide and can support policy-makers and

689 farmers to establish suitable strategies to limit damage related to soil salinity. The outcome of this research is as

690 follows.

691 - This study justified the effectiveness of machine learning and remote sensing in soil salinity monitoring in the Red

692 River Delta. The results of this study can be opened to realize in different regions.

693 - Five optimization algorithms, namely POA, STO, SOA, PSO, and GOA, were successful in optimizing the accuracy

694 of the XGB model. All these algorithms were successful in improving the accuracy of XGB. Of these, the XGB-POA

695 model showed the greatest performance, with an R^2 value of 0.968. This was followed by XGB-STO (R^2=0.967),

696 XGB-SOA (R^2=0.966), XGB-PSO (R^2=0.964), and XGB-GOA (R^2=0.964).

697 - The models in this research were utilized to construct soil salinity maps. The maps demonstrated that littoral areas

698 and those along the rivers were the most influenced by the soil salinity problem because these regions are influenced

699 by seawater. In addition, when the river levels are lower during the dry season, it creates the conditions for seawater

700 to penetrate the land.

701 - Five factors were analyzed to consider farmers' adaptive capacity: natural capital, human capital, material resources,

702 financial resources, and social capital. The results show that people have awareness and actions in improving their

703 adaptive capacity to increasingly severe saline intrusion; however, there are still many limitations related to lack of

704 awareness and finance. As a recommendation, the participation of multiple stakeholders is required, with a particular

705 emphasis on the role of policies in sustainably and effectively enhancing people's adaptive capacity.

706 The outcome of this research provides key knowledge on the spatial distribution of soil salinity and farmers' adaptive

707 capacity to growing salinization, to support local authorities or farmers in proposing appropriate measures to reduce

708 soil salinity damage. This can complement a theoretical framework in the existing literature on soil salinity

709 management and adaptive capacity.

710 **Statements and Declarations**

711 **Funding**

712 This research is funded by Vietnam National Foundation for Science and Technology Development (NAFOSTED)
713 under grant number 105.08-2023.13

714 **Competing Interests**

715 The authors declare that they have no conflict of interest.

716 **Ethics and consent to participate**

717 Not applicable

718 **Consent for publication**

719 Not applicable

720 **Authors Contributions**

721 **Huu Duy Nguyen:** Conceptualization, Formal analysis, Funding acquisition, Investigation, Methodology,
722 Supervision, Writing – original draft, Writing – review & editing. **Quang-Thanh Bui:** Conceptualization,
723 Formal analysis, Investigation, Methodology, Supervision, Writing – original draft, Writing – review &
724 editing. **Thi Anh Tam Lai:** Data curation**. Duc Dung Tran:** Data curation, Investigation, Writing –
725 original draft, Writing – review & editing. **Dinh Kha Dang:** Data curation, Investigation. **Himan
726 Shahabi:** Writing – original draft, Writing – review & editing.

727 **Availability of data and materials**

728 The datasets used and/or analysed during the current study available from the corresponding author on reasonable
729 request

730 **Reference**

731 Aksoy, S., Sertel, E., Roscher, R., Tanik, A., Hamzehpour, N., 2024. Assessment of soil salinity using
732   explainable machine learning methods and Landsat 8 images. International Journal of Applied
733   Earth Observation and Geoinformation 130, 103879.
734 Al-Sarray, N.H.S., Rahebi, J., Demirhan, A., 2024. Detection of DDoS attacks in SDN with Siberian Tiger
735   Optimization algorithm and deep learning.
736 Alamir, N., Kamel, S., Megahed, T.F., Hori, M., Abdelkader, S.M., 2023. Developing hybrid demand
737   response technique for energy management in microgrid based on pelican optimization
738   algorithm. Electric Power Systems Research 214, 108905.
739 Asfaw, E., Suryabhagavan, K., Argaw, M., 2018. Soil salinity modeling and mapping using remote sensing
740   and GIS: The case of Wonji sugar cane irrigation farm, Ethiopia. Journal of the Saudi Society of
741   Agricultural Sciences 17(3), 250-258.
742 Bandak, S., Movahedi-Naeini, S.A., Mehri, S., Lotfata, A., 2024. A longitudinal analysis of soil salinity
743   changes using remotely sensed imageries. Scientific Reports 14(1), 10383.
744 Bhuyan, M.I., Supit, I., Kumar, U., Mia, S., Ludwig, F., 2024. The significance of farmers' climate change
745   and salinity perceptions for on-farm adaptation strategies in the south-central coast of
746   Bangladesh. Journal of Agriculture and Food Research 16, 101097.
747 Bui, D.T., Pradhan, B., Nampak, H., Bui, Q.-T., Tran, Q.-A., Nguyen, Q.-P., 2016. Hybrid artificial intelligence
748   approach based on neural fuzzy inference model and metaheuristic optimization for flood
749   susceptibiligy modeling in a high-frequency tropical cyclone area using GIS. Journal of Hydrology
750   540, 317-330.
751 Castelletti, A., Pianosi, F., Quach, X., Soncini-Sessa, R., 2012. Assessing water reservoirs management and
752   development in Northern Vietnam. Hydrology and Earth System Sciences 16(1), 189-199.
753 Cullu, M.A., 2003. Estimation of the effect of soil salinity on crop yield using remote sensing and
754   geographic information system. Turkish Journal of Agriculture and Forestry 27(1), 23-28.
755 Dasgupta, S., Laplante, B., Murray, S., Wheeler, D., 2009. Climate change and the future impacts of storm-
756   surge disasters in developing countries. Center for Global Development Working Paper (182).
757 Dehghani, M., Trojovský, P., 2022. Serval optimization algorithm: a new bio-inspired approach for solving
758   optimization problems. Biomimetics 7(4), 204.
759 Du, L., Tian, S., Zhao, N., Zhang, B., Mu, X., Tang, L., Zheng, X., Li, Y., 2024. Climate and topography regulate
760   the spatial pattern of soil salinization and its effects on shrub community structure in Northwest
761   China. Journal of Arid Land, 1-18.
762 Eldeiry, A.A., Garcia, L.A., Reich, R.M., 2008. Soil salinity sampling strategy using spatial modeling
763   techniques, remote sensing, and field data. Journal of irrigation and drainage engineering 134(6),
764   768-777.
765 Elshewy, M.A., Mohamed, M.H., Refaat, M., 2024. Developing a soil salinity model from landsat 8 satellite
766   bands based on advanced machine learning algorithms. Journal of the Indian Society of Remote
767   Sensing 52(3), 617-632.
768 Fathizad, H., Ardakani, M.A.H., Sodaiezadeh, H., Kerry, R., Taghizadeh-Mehrjardi, R., 2020. Investigation
769   of the spatial and temporal variation of soil salinity using random forests in the central desert of
770   Iran. Geoderma 365, 114233.
771 Fu, C., Gan, S., Yuan, X., Xiong, H., Tian, A., 2018. Determination of soil salt content using a probability
772   neural network model based on particle swarm optimization in areas affected and non-affected
773   by human activities. Remote Sensing 10(9), 1387.
774 Gong, Z., He, H., Fan, D., Sheng, J., Zhang, X., 2023. Inversion of sea surface salinity in Bay of Bengal based
775   on Catboost algorithm, Second International Conference on Geographic Information and Remote
776   Sensing Technology (GIRST 2023). SPIE, pp. 297-304.
777 Hardie, M., Doyle, R., 2012. Measuring soil salinity. Plant salt tolerance: methods and protocols, 415-425.

He, Y., Yin, H., Chen, Y., Xiang, R., Zhang, Z., Chen, H., 2024. Soil Salinity Estimation based on Sentinel-1/2 Texture Features and Machine Learning. IEEE Sensors Journal.

Hien, N.T., Yen, N.H., Balistrocchi, M., Peli, M., Cat, V.M., Ranzi, R., 2023. Salinity dynamics under different water management plans coupled with sea level rise scenarios in the Red River Delta, Vietnam. Journal of Hydro-environment Research 51, 67-81.

Hoa, P.V., Giang, N.V., Binh, N.A., Hai, L.V.H., Pham, T.-D., Hasanlou, M., Tien Bui, D., 2019. Soil salinity mapping using SAR sentinel-1 data and advanced machine learning algorithms: A case study at Ben Tre Province of the Mekong River Delta (Vietnam). Remote Sensing 11(2), 128.

Hoang, L.P., Pot, M., Tran, D.D., Ho, L.H., Park, E., 2023. Adaptive capacity of high- and low dyke farmers to hydrological changes in the Vietnamese Mekong delta. Environmental Research 224, 115423.

Hoang, N.K., Hai, D.T., 2024. Assessing surface water salinity intrusion in the Mekong River Delta: a case study in Rach Gia, Vietnam. GeoJournal 89(4), 171.

Hung, N.M., Larson, M., 2014. Coastline and river mouth evolution in the central part of the Red River Delta, Coastal disasters and climate change in Vietnam. Elsevier, pp. 43-79.

Ingle, K.K., Jatoth, R.K., 2024. Non-linear Channel Equalization using Modified Grasshopper Optimization Algorithm. Applied Soft Computing 153, 110091.

Jia, P., Zhang, J., Liang, Y., Zhang, S., Jia, K., Zhao, X., 2024. The inversion of arid-coastal cultivated soil salinity using explainable machine learning and Sentinel-2. Ecological Indicators 166, 112364.

Jiang, H., Rusuli, Y., Amuti, T., He, Q., 2019. Quantitative assessment of soil salinity using multi-source remote sensing data based on the support vector machine and artificial neural network. International journal of remote sensing 40(1), 284-306.

Juneja, M., Nagar, S., 2016. Particle swarm optimization algorithm and its parameters: A review, 2016 International Conference on Control, Computing, Communication and Materials (ICCCCM). IEEE, pp. 1-5.

Kaplan, G., Gašparović, M., Alqasemi, A.S., Aldhaheri, A., Abuelgasim, A., Ibrahim, M., 2023. Soil salinity prediction using Machine Learning and Sentinel – 2 Remote Sensing Data in Hyper – Arid areas. Physics and Chemistry of the Earth, Parts A/B/C 130, 103400.

Kennedy, J., Eberhart, R., 1995. Particle swarm optimization, Proceedings of ICNN'95-international conference on neural networks. ieee, pp. 1942-1948.

Le Dang, H., Li, E., Nuberg, I., Bruwer, J., 2014. Understanding farmers' adaptation intention to climate change: A structural equation modelling study in the Mekong Delta, Vietnam. Environmental science & policy 41, 11-22.

Li, S., Zhang, T., Yu, J., 2023. Photovoltaic array dynamic reconfiguration based on an improved pelican optimization algorithm. Electronics 12(15), 3317.

Liu, W., Chen, Z., Hu, Y., 2022. XGBoost algorithm-based prediction of safety assessment for pipelines. International Journal of Pressure Vessels and Piping 197, 104655.

Liu, Y., Han, X., Zhu, Y., Li, H., Qian, Y., Wang, K., Ye, M., 2024. Spatial mapping and driving factor Identification for salt-affected soils at continental scale using Machine learning methods. Journal of Hydrology 639, 131589.

Ma, G., Ding, J., Han, L., Zhang, Z., Ran, S., 2021. Digital mapping of soil salinization based on Sentinel-1 and Sentinel-2 data combined with machine learning algorithms. Regional Sustainability 2(2), 177-188.

Mazumder, M.S.U., Kabir, M.H., 2022. Farmers' adaptations strategies towards soil salinity effects in agriculture: the interior coast of Bangladesh. Climate Policy 22(4), 464-479.

Mirjalili, S.Z., Mirjalili, S., Saremi, S., Faris, H., Aljarah, I., 2018. Grasshopper optimization algorithm for multi-objective optimization problems. Applied Intelligence 48, 805-820.

Mo, H., Sun, H., Liu, J., Wei, S., 2019. Developing window behavior models for residential buildings using XGBoost algorithm. Energy and Buildings 205, 109564.

Moayedi, H., Gör, M., Lyu, Z., Bui, D.T., 2020. Herding Behaviors of grasshopper and Harris hawk for hybridizing the neural network in predicting the soil compression coefficient. Measurement 152, 107389.

Moayedi, H., Nguyen, H., Kok Foong, L., 2021. Nonlinear evolutionary swarm intelligence of grasshopper optimization algorithm and gray wolf optimization for weight adjustment of neural network. Engineering with Computers 37(2), 1265-1275.

Mukhamediev, R.I., Merembayev, T., Kuchin, Y., Malakhov, D., Zaitseva, E., Levashenko, V., Popova, Y., Symagulov, A., Sagatdinova, G., Amirgaliyev, Y., 2023. Soil Salinity Estimation for South Kazakhstan Based on SAR Sentinel-1 and Landsat-8, 9 OLI Data with Machine Learning Models. Remote Sensing 15(17), 4269.

Nguyen, H.D., 2022. Hybrid models based on deep learning neural network and optimization algorithms for the spatial prediction of tropical forest fire susceptibility in Nghe An province, Vietnam. Geocarto International 37(26), 11281-11305.

Nguyen, H.D., Van, C.P., Nguyen, T.G., Dang, D.K., Pham, T.T.N., Nguyen, Q.-H., Bui, Q.-T., 2023. Soil salinity prediction using hybrid machine learning and remote sensing in Ben Tre province on Vietnam's Mekong River Delta. Environmental Science and Pollution Research, 1-18.

Nguyen, M.T., Renaud, F.G., Sebesvari, Z., 2019. Drivers of change and adaptation pathways of agricultural systems facing increased salinity intrusion in coastal areas of the Mekong and Red River deltas in Vietnam. Environmental science & policy 92, 331-348.

Nguyen, P.T., Koedsin, W., McNeil, D., Van, T.P., 2018. Remote sensing techniques to predict salinity intrusion: application for a data-poor area of the coastal Mekong Delta, Vietnam. International journal of remote sensing 39(20), 6676-6691.

Nguyen, Q.H., Takewaka, S., 2020. Land subsidence and its effects on coastal erosion in the Nam Dinh Coast (Vietnam). Continental Shelf Research 207, 104227.

Nguyen, T.G., Tran, N.A., Vu, P.L., Nguyen, Q.-H., Nguyen, H.D., Bui, Q.-T., 2021. Salinity intrusion prediction using remote sensing and machine learning in data-limited regions: A case study in Vietnam's Mekong Delta. Geoderma Regional 27, e00424.

Nguyen, V.H., Germer, J., Asch, F., 2024. Evaluating topsoil salinity via geophysical methods in rice production systems in the Vietnam Mekong Delta. Journal of Agronomy and Crop Science 210(1), e12676.

Nguyen, Y.T.B., Kamoshita, A., Dinh, V.T.H., Matsuda, H., Kurokura, H., 2017. Salinity intrusion and rice production in Red River Delta under changing climate conditions. Paddy and Water Environment 15, 37-48.

Nhuan, M.T., Van Ngoi, C., Nghi, T., Tien, D.M., van Weering, T.C., van den Bergh, G., 2007. Sediment distribution and transport at the nearshore zone of the Red River delta, Northern Vietnam. Journal of Asian Earth Sciences 29(4), 558-565.

Premkumar, N., Santhosh, R., 2024. Pelican optimization algorithm with blockchain for secure load balancing in fog computing. Multimedia Tools and Applications 83(18), 53417-53439.

Quang, N.H., Viet, T.Q., Thang, H.N., Hieu, N.T.D., 2024. Long-term water level dynamics in the Red River basin in response to anthropogenic activities and climate change. Science of The Total Environment 912, 168985.

Ramraj, S., Uzir, N., Sunil, R., Banerjee, S., 2016. Experimenting XGBoost algorithm for prediction and classification of different datasets. International Journal of Control Theory and Applications 9(40), 651-662.

Rhoades, J., Ingvalson, R., 1971. Determining salinity in field soils with soil resistance measurements. Soil Science Society of America Journal 35(1), 54-60.

Rini, D.P., Shamsuddin, S.M., Yuhaniz, S.S., 2011. Particle swarm optimization: technique, system and challenges. International journal of computer applications 14(1), 19-26.

874 Ruidas, D., Chakrabortty, R., Islam, A.R.M.T., Saha, A., Pal, S.C., 2022. A novel hybrid of meta-optimization
875   approach for flash flood-susceptibility assessment in a monsoon-dominated watershed, Eastern
876   India. Environmental earth sciences 81(5), 145.
877 Shi, H., Hellwich, O., Luo, G., Chen, C., He, H., Ochege, F.U., Van de Voorde, T., Kurban, A., De Maeyer, P.,
878   2021. A global meta-analysis of soil salinity prediction integrating satellite remote sensing, soil
879   sampling, and machine learning. IEEE Transactions on Geoscience and Remote Sensing 60, 1-15.
880 Sindi, A.O.N., Si, P., Li, Q., 2024. Secure Task Offloading and Resource Allocation Strategies in Mobile
881   Applications Using Probit Mish-Gated Recurrent Unit and an Enhanced-Searching-Based Serval
882   Optimization Algorithm. Electronics 13(13), 2462.
883 Song, Y., Gao, M., Wang, J., 2024. Inversion of salinization in multilayer soils and prediction of water
884   demand for salt regulation in coastal region. Agricultural Water Management 301, 108970.
885 Su, Y., Li, T., Cheng, S., Wang, X., 2020. Spatial distribution exploration and driving factor identification for
886   soil salinisation based on geodetector models in coastal area. Ecological Engineering 156, 105961.
887 Tan, J., Ding, J., Han, L., Ge, X., Wang, X., Wang, J., Wang, R., Qin, S., Zhang, Z., Li, Y., 2023. Exploring
888   planetScope satellite capabilities for soil salinity estimation and mapping in arid regions oases.
889   Remote Sensing 15(4), 1066.
890 Thiam, H.I., Owusu, V., Villamor, G.B., Schuler, J., Hathie, I., 2024. Farmers' intention to adapt to soil
891   salinity expansion in Fimela, Sine-Saloum area in Senegal: A structural equation modelling
892   approach. Land Use Policy 137, 106990.
893 Tran, V.N., Kim, J., 2022. Robust and efficient uncertainty quantification for extreme events that deviate
894   significantly from the training dataset using polynomial chaos-kriging. Journal of Hydrology 609,
895   127716.
896 Trojovský, P., Dehghani, M., 2022. Pelican optimization algorithm: A novel nature-inspired algorithm for
897   engineering applications. Sensors 22(3), 855.
898 Trojovský, P., Dehghani, M., Hanuš, P., 2022. Siberian tiger optimization: A new bio-inspired metaheuristic
899   algorithm for solving engineering optimization problems. Ieee Access 10, 132396-132431.
900 Vermeulen, D., Van Niekerk, A., 2017. Machine learning performance for predicting soil salinity using
901   different combinations of geomorphometric covariates. Geoderma 299, 1-12.
902 Vinh, V.D., Ouillon, S., Thanh, T.D., Chu, L., 2014. Impact of the Hoa Binh dam (Vietnam) on water and
903   sediment budgets in the Red River basin and delta. Hydrology and Earth System Sciences 18(10),
904   3987-4005.
905 Wang, H., Hsieh, Y.P., Harwell, M.A., Huang, W., 2007. Modeling soil salinity distribution along topographic
906   gradients in tidal salt marshes in Atlantic and Gulf coastal regions. Ecological modelling 201(3-4),
907   429-439.
908 Wang, H., Zhang, L., Zhao, J., Hu, X., Ma, X., 2022. Application of hyperspectral technology combined with
909   bat algorithm-AdaBoost model in field soil nutrient prediction. Ieee Access 10, 100286-100299.
910 Wang, J., Peng, J., Li, H., Yin, C., Liu, W., Wang, T., Zhang, H., 2021. Soil salinity mapping using machine
911   learning algorithms with the Sentinel-2 MSI in arid areas, China. Remote Sensing 13(2), 305.
912 Wang, J., Wang, X., Zhang, J., Shang, X., Chen, Y., Feng, Y., Tian, B., 2024. Soil Salinity Inversion in Yellow
913   River Delta by Regularized Extreme Learning Machine Based on ICOA. Remote Sensing 16(9),
914   1565.
915 Wang, W., Sun, J., 2024. Estimation of soil salinity using satellite-based variables and machine learning
916   methods. Earth Science Informatics, 1-13.
917 Wu, W., Zucca, C., Muhaimeed, A.S., Al-Shafie, W.M., Fadhil Al-Quraishi, A.M., Nangia, V., Zhu, M., Liu, G.,
918   2018. Soil salinity prediction and mapping by machine learning regression in C entral M
919   esopotamia, I raq. Land degradation & development 29(11), 4005-4014.

920   Xiao, C., Ji, Q., Chen, J., Zhang, F., Li, Y., Fan, J., Hou, X., Yan, F., Wang, H., 2023. Prediction of soil salinity
921   parameters using machine learning models in an arid region of northwest China. Computers and
922   Electronics in Agriculture 204, 107512.
923   Xiao, S., Nurmemet, I., Zhao, J., 2024. Soil salinity estimation based on machine learning using the GF-3
924   radar and Landsat-8 data in the Keriya Oasis, Southern Xinjiang, China. Plant and Soil 498(1), 451-
925   469.
926   Xie, J., Shi, C., Liu, Y., Wang, Q., Zhong, Z., Wang, X., He, S., Feature Variable Selection Methods for
927   Inversion of Soil Salinity at the Irrigation District Scale Based on Machine Learning. Available at
928   SSRN 4865442.
929   Yuen, K.W., Hanh, T.T., Quynh, V.D., Switzer, A.D., Teng, P., Lee, J.S.H., 2021. Interacting effects of land-
930   use change and natural hazards on rice agriculture in the Mekong and Red River deltas in Vietnam.
931   Natural Hazards and Earth System Sciences 21(5), 1473-1493.
932   Zhang, W., Zhang, W., Liu, Y., Zhang, J., Yang, L., Wang, Z., Mao, Z., Qi, S., Zhang, C., Yin, Z., 2022. The role
933   of soil salinization in shaping the spatio-temporal patterns of soil organic carbon stock. Remote
934   Sensing 14(13), 3204.
935   Zhao, R., Ni, H., Feng, H., Song, Y., Zhu, X., 2019. An improved grasshopper optimization algorithm for task
936   scheduling problems. Int. J. Innov. Comput., Inf. Control 15, 1967-1987.

937

938